Dynamic many-body theory: Dynamics of strongly correlated Fermi fluids

H. M. Böhm,[1] R. Holler,[1] E. Krotscheck,[1,2] and M. Panholzer[1]
[1]*Institut für Theoretische Physik, Johannes Kepler Universität, A 4040 Linz, Austria*
[2]*Department of Physics, University at Buffalo–SUNY, Buffalo, New York 14260, USA*
(Received 23 August 2010; revised manuscript received 23 October 2010; published 6 December 2010)

We develop a systematic theory of multiparticle excitations in strongly interacting Fermi systems. Our work is the generalization of the time-honored work by Jackson, Feenberg, and Campbell for bosons, that provides, in its most advanced implementation, quantitative predictions for the dynamic structure function in the whole experimentally accessible energy/momentum regime. Our view is that the same physical effects, namely, fluctuations of the wave function at an atomic length scale are responsible for the correct energetics of the excitations in both Bose and Fermi fluids. Besides a comprehensive derivation of the fermion version of the theory and discussion of the approximations made, we present results for homogeneous ^{3}He and electrons in three dimensions. We find indeed a significant lowering of the zero-sound mode in ^{3}He and a broadening of the collective mode due to the coupling to two-particle–two-hole excitations in good agreement with experiments. The most visible effect in electronic systems is the appearance of a "double-plasmon" excitation.

DOI: 10.1103/PhysRevB.82.224505 PACS number(s): 67.30.em, 71.10.Ca, 71.15.Qe

I. INTRODUCTION

This paper is concerned with a systematic theory of multiparticle excitations in Fermi systems. We utilize an equations-of-motion method that has been used in the past as a vehicle for many purposes: the derivation of the time-dependent Hartree-Fock (TDHF) theory,[1–3] its analog for strongly interacting systems,[4,5] and for studying single-particle and multiparticle correlations in strongly interacting Bose liquids.[6,7]

The simplest way to deal with excitations is to assume that the low-lying excited states of a quantum fluid can be characterized by the quantum numbers of a single particle. This is the core idea of Landau's quasiparticle picture of "normal" quantum fluids[8,9] as well as of Feynman's theory of collective modes in the helium liquids.[10] It is appropriate for many long-wavelengths excitations such as sound waves in Bose fluids or plasmons in an electron liquid.

Already Feynman realized that this concept is insufficient to describe higher lying excitations, most prominently the "roton" in ^{4}He. Intuitively appealing, he introduced "backflow" correlations.[11] These are recognizable as a new type of excitations, depending on two particles: *pair fluctuations*. The notion is plausible for excitations at wavelengths comparable to the interparticle distance, the time dependence of a system's *short-ranged* structure is expected to be relevant.

The presently state-of-the-art theory for Bose liquids originates from pioneering studies by Jackson, Feenberg,[6,12–16] and Campbell and collaborators.[17] Recently, a complete solution of the pair equation of motion has been accomplished in ^{4}He,[7] showing that the "uniform limit approximation" of Refs. 6 and 12–17 is surprisingly good. Consequently, theoretical improvement must be sought in three-body and higher-order fluctuations.[18]

Although quite successful for bosons, there exists to-date no fermion version of the theory. We therefore develop here the generalization of the equation-of-motion method for pair fluctuations to fermions. We calculate the fermionic density-density response function $\chi(\mathbf{r}-\mathbf{r}';t-t')$, relating the induced density fluctuation $\delta\rho(\mathbf{r};t)$ to a weak external perturbation $h_{\rm ext}(\mathbf{r};t)$. In a homogeneous system this is written in momentum space as

$$\delta\rho(\mathbf{q};\omega) = \rho\chi(q;\omega)\tilde{h}_{\rm ext}(\mathbf{q};\omega), \tag{1.1}$$

where ρ is the particle number N per volume Ω. We choose Fourier transforms

$$f(\mathbf{r};\omega) \equiv \frac{1}{N}\sum_{\mathbf{q}} e^{-i\mathbf{q}\cdot\mathbf{r}}\tilde{f}(\mathbf{q};\omega) \tag{1.2}$$

to have the same dimension in $\mathbf{q}$ and $\mathbf{r}$ spaces.

The imaginary part of $\chi(q;\omega)$ is the experimentally accessible dynamic structure factor,

$$S(q;\omega) = -\frac{\hbar}{\pi}\Im m[\chi(q;\omega)]\theta(\omega). \tag{1.3}$$

The dynamic structure factor satisfies, among others, the sum rules

$$m_0 = S(q) = \int_0^\infty d(\hbar\omega)S(q;\omega), \tag{1.4}$$

$$m_1 = \frac{\hbar^2 q^2}{2m} = \int_0^\infty d(\hbar\omega)\hbar\omega S(q;\omega), \tag{1.5}$$

where $S(q)$ is the static structure factor.

We develop our theory with the following objectives.

(1) Technically, the extension of the Jackson-Feenberg-Campbell theory to Fermi systems amounts to including time-dependent *two-particle-two-hole* excitations. We require that the fermionic $\chi(q;\omega)$ reduces to that of the boson theory in the appropriate limit.

(2) For bosons, neglecting pair-order and higher order fluctuations yields the famous Bijl-Feynman spectrum[10]

$$\varepsilon(q) = \frac{\hbar^2 q^2}{2mS(q)} \equiv \frac{t(q)}{S(q)}. \tag{1.6}$$

Its fermionic counterpart is the random-phase approximation (RPA), formulated in terms of effective interactions.[19] We require that our theory reduces to the RPA if pair fluctuations are ignored. This implies, in particular, that we obtain in this case a response function of the form

$$\chi(q;\omega) = \frac{\chi_0(q;\omega)}{1 - \tilde{V}_{\text{p-h}}(q)\chi_0(q;\omega)}. \tag{1.7}$$

Here, $\chi_0(q;\omega)$ is the Lindhard function and $\tilde{V}_{\text{p-h}}(q)$ an appropriately defined static "particle-hole interaction" or "pseudopotential."

One of the tasks of microscopic many-body theory is to justify and calculate effective interactions such as $\tilde{V}_{\text{p-h}}(q)$, as far as this is possible. Using Jastrow-Feenberg-correlation functions[13] to tame the microscopic hard-core repulsion, it has been shown[5] under what assumptions a density response function of the RPA form Eq. (1.7) can be obtained, and a microscopic expression for the static effective interaction $\tilde{V}_{\text{p-h}}(q)$ was derived. Under what conditions a form Eq. (1.7) is meaningful at all will be discussed in depth below.

A phenomenological approach to define a particle-hole interaction or pseudopotential for ^{3}He and electrons was introduced by Aldrich, Iwamoto, and Pines.[19,20] They determined the physically intuitive and necessary requirements for $\tilde{V}_{\text{p-h}}(q)$, postulating that the dynamic response is given by the RPA form Eq. (1.7). Reflecting the same physics, the $\tilde{V}_{\text{p-h}}(q)$ derived from microscopic many-body theory[5] is very similar to the Aldrich-Iwamoto-Pines pseudopotentials. The microscopic derivation leads to a $\tilde{V}_{\text{p-h}}(q)$ that is uniquely determined from the static structure function by the two sum rules in Eqs. (1.4) and (1.5). Defining the RPA this way leads for bosons to the Feynman approximation Eq. (1.6) for the spectrum of collective excitations. From here on, we will use the term "RPA" and Feynman spectrum in this sense.

Our work is organized as follows. Section II introduces the basic quantities and the most important tools of variational and correlated basis function (CBF) theory. For details, the reader is referred to review articles[21] and pedagogical material;[22] a brief outline of our notations and definitions is given in Appendix A. Section III is the core of our work; it provides the derivation of the equations of motion, including pair fluctuations. We show that the theory can be mapped onto a set of TDHF equations[3] with *energy-dependent, effective* interactions. Thus, our work provides the logical generalization of Ref. 5, where single-particle fluctuations led to a TDHF theory with *static* effective interactions.

Section IV focuses on the practical implementation of our theory. We formulate, among others, the "convolution approximation" for fermions. In Sec. V we derive the density-density response function $\chi(q;\omega)$ and discuss its features.

Modern techniques of many-body theory are robust against the details of the interparticle interaction. We can therefore use the methods developed here to examine the dynamics of two very different systems: The very strongly interacting ^{3}He whose interaction is characterized by a repulsive hard core and a short-ranged attraction, and electrons with their rather tame but long-ranged Coulomb interaction. Section VI implements our method for bulk ^{3}He and the electron liquid. In ^{3}He, we compare with neutron-scattering experiments carried out at the Institut Laue Langevin (ILL) in the group led by Scherm.[23–25] The energetics of the collective mode as well as the width of the spectrum at high-momentum transfers are significantly improved compared to RPA predictions. In the homogeneous electron liquid the pair-excitation theory predicts plasmon damping as well as double-plasmon excitations. Experimental verification of the double-plasmon excitation in recent inelastic X-ray scattering measurements[26,27] has added new interest in studying the dynamics of electrons.

Our results are summarized in Sec. VII where we also discuss the directions of future work. Appendices A and E give further details on the derivations and Appendix F a very brief summary of the minimal implementation of our theory.

II. THEORY FOR STRONGLY INTERACTING FERMIONS

A. Variational theory

Microscopic many-body theory starts with a phenomenological Hamiltonian for N interacting fermions,

$$H = -\sum_i \frac{\hbar^2}{2m}\nabla_i^2 + \sum_{i<j} v(|\mathbf{r}_i - \mathbf{r}_j|). \tag{2.1}$$

For strong interactions, CBF theory[13] has proved to be an efficient and accurate method for obtaining ground-state properties. It starts with a variational wave function of the form

$$|\Psi_{\mathbf{o}}\rangle = \frac{F|\Phi_{\mathbf{o}}\rangle}{\langle\Phi_{\mathbf{o}}|F^\dagger F|\Phi_{\mathbf{o}}\rangle^{1/2}}, \tag{2.2}$$

where $\Phi_{\mathbf{o}}(1,\ldots,i,\ldots,N)$ is a model state, normally a Slater determinant, and "i" is short for both spatial and ν discrete (spin and/or isospin) degrees of freedom. The *correlation operator* $F(1,\ldots,N)$ is suitably chosen to describe the important features of the interacting system. Most practical and highly successful is the Jastrow-Feenberg[13] form

$$F(1,\ldots,N) = \exp\left\{\frac{1}{2}\sum_{1\le i<j\le N} u_2(\mathbf{r}_i,\mathbf{r}_j) + \frac{1}{2}\sum_{1\le i<j<k\le N} u_3(\mathbf{r}_i,\mathbf{r}_j,\mathbf{r}_k) + \cdots\right\}. \tag{2.3}$$

The $u_n(\mathbf{r}_1,\ldots,\mathbf{r}_n)$ are made unique by requiring them to vanish for $|\mathbf{r}_i - \mathbf{r}_j| \to \infty$ "cluster property."

From the wave function Eqs. (2.2) and (2.3), the energy expectation value

$$H_{\mathbf{o},\mathbf{o}} \equiv \langle\Psi_{\mathbf{o}}|H|\Psi_{\mathbf{o}}\rangle \tag{2.4}$$

can be calculated either by simulation or by integral equation methods. The hierarchy of Fermi-Hypernetted-Chain (FHNC) approximations is compatible with the optimization

problem, i.e., with determining the optimal *correlation functions* $u_n(\mathbf{r}_1,\ldots,\mathbf{r}_n)$ through functionally minimizing the energy

$$\frac{\delta H_{\mathbf{o},\mathbf{o}}}{\delta u_n(\mathbf{r}_1,\ldots,\mathbf{r}_n)}=0. \tag{2.5}$$

Due to the multitude of exchange diagrams, the FHNC and corresponding Euler equations (FHNC-EL) can be quite complicated;[28] the simplest approximation of the Euler Eq. (2.5) that contains the important physics is spelled out in Appendix A 1.

The optimization of the correlations also facilitates making connections with other types of many-body theories, such as Feynman-diagram-based expansions and summations.[29]

B. Correlated basis functions

Although quite successful in predicting ground-state properties of strongly interacting systems, the Jastrow-Feenberg form Eq. (2.3) of the correlation operator F has some deficiencies. The most obvious problem is that the nodes of the wave function Eq. (2.2) are identical to those of the model state $|\Phi_\mathbf{o}\rangle$. To improve upon the description of physics, CBF theory[21,22,28] uses the correlation operator F to generate a complete set of correlated and normalized N-particle basis states through

$$|\Psi_\mathbf{m}\rangle=\frac{F|\Phi_\mathbf{m}\rangle}{\langle\Phi_\mathbf{m}|F^\dagger F|\Phi_\mathbf{m}\rangle^{1/2}}, \tag{2.6}$$

where the $\{|\Phi_\mathbf{m}\rangle\}$ form a complete basis of model states. Although the $|\Psi_\mathbf{m}\rangle$ are not orthogonal, perturbation theory can be formulated in terms of these states.[13,30] We review here this method only very briefly, details may be found in Refs. 21 and 22; the diagrammatic construction of the relevant ingredients is given in Ref. 31.

For economy of notation, we introduce a "second-quantized" formulation of the correlated states. The Jastrow-Feenberg-correlation operator in Eq. (2.3) explicitly depends on the particle number, i.e., $F=F_N(1,\ldots,N)$ (whenever unambiguous, we omit the corresponding subscript). Starting from the conventional $a_k^\dagger, a_k$, creation and annihilation operators $\alpha_k^\dagger, \alpha_k$ of *correlated states* are defined by their action on the basis states

$$\alpha_k^\dagger|\Psi_\mathbf{m}\rangle\equiv\frac{F_{N+1}a_k^\dagger|\Phi_\mathbf{m}\rangle}{\langle\Phi_\mathbf{m}|a_k F_{N+1}^\dagger F_{N+1}a_k^\dagger|\Phi_\mathbf{m}\rangle^{1/2}}, \tag{2.7}$$

$$\alpha_k|\Psi_\mathbf{m}\rangle\equiv\frac{F_{N-1}a_k|\Phi_\mathbf{m}\rangle}{\langle\Phi_\mathbf{m}|a_k^\dagger F_{N-1}^\dagger F_{N-1}a_k|\Phi_\mathbf{m}\rangle^{1/2}}. \tag{2.8}$$

According to these definitions, $\alpha_k^\dagger$ and α_k obey the same (anti)commutation rules as the creation and annihilation operators $a_k^\dagger$ and a_k of uncorrelated states, *but they are not Hermitian conjugates*. If $|\Psi_\mathbf{m}\rangle$ is an N-particle state, then the state in Eq. (2.7) must carry an $(N+1)$-particle correlation operator while that in Eq. (2.8) must be formed with an $(N-1)$-particle correlation operator.

In general, we label "hole" states, which are occupied in $|\Phi_\mathbf{o}\rangle$, by h, h', h_i,…, and unoccupied "particle" states by p, p', p_i, etc. To display the particle-hole pairs explicitly, we will alternatively to $|\Psi_\mathbf{m}\rangle$ use the notation $|\Psi_{p_1,\ldots,p_d h_1,\ldots,h_d}\rangle$. A basis state with d particle-hole pairs is then

$$|\Psi_{p_1,\ldots,p_d h_1,\ldots,h_d}\rangle=\alpha_{p_1}^\dagger\ldots\alpha_{p_d}^\dagger\alpha_{h_d}\ldots\alpha_{h_1}|\Psi_\mathbf{o}\rangle. \tag{2.9}$$

The execution of the theory needs the matrix elements of the Hamiltonian, the unit operator and the density operator. Key quantities are diagonal and off-diagonal matrix elements of unity and $H'\equiv H-H_{\mathbf{o},\mathbf{o}}$

$$M_{\mathbf{m},\mathbf{n}}=\langle\Psi_\mathbf{m}|\Psi_\mathbf{n}\rangle\equiv\delta_{\mathbf{m},\mathbf{n}}+N_{\mathbf{m},\mathbf{n}}, \tag{2.10}$$

$$H'_{\mathbf{m},\mathbf{n}}\equiv W_{\mathbf{m},\mathbf{n}}+\frac{1}{2}(H_{\mathbf{m},\mathbf{m}}+H_{\mathbf{n},\mathbf{n}}-2H_{\mathbf{o},\mathbf{o}})N_{\mathbf{m},\mathbf{n}}. \tag{2.11}$$

Equation (2.11) defines a natural decomposition[31,32] of the matrix elements of $H'_{\mathbf{m},\mathbf{n}}$ into the off-diagonal quantities $W_{\mathbf{m},\mathbf{n}}$ and $N_{\mathbf{m},\mathbf{n}}$ and diagonal quantities $H_{\mathbf{m},\mathbf{m}}$.

The ratios of normalization integrals, $I_{\mathbf{m},\mathbf{m}}\equiv\langle\Phi_\mathbf{m}|F^\dagger F|\Phi_\mathbf{m}\rangle$, define the factors

$$z_{p_1,\ldots,p_d h_1,\ldots,h_d}\equiv z_\mathbf{m}\equiv\sqrt{I_{\mathbf{m},\mathbf{m}}/I_{\mathbf{o},\mathbf{o}}}. \tag{2.12}$$

For large particle numbers and $d\ll N$ these factorize as

$$z_\mathbf{m}=\frac{z_{p_1}\cdots z_{p_d}}{z_{h_1}\cdots z_{h_d}}+\mathcal{O}(N^{-1}). \tag{2.13}$$

Likewise, to leading order in the particle number, the *diagonal* matrix elements of $H'\equiv H-H_{\mathbf{o},\mathbf{o}}$ become additive so that for the above d-pair state we can define the CBF single-particle energies

$$\langle\Psi_\mathbf{m}|H'|\Psi_\mathbf{m}\rangle\equiv\sum_{i=1}^{d}e_{p_i h_i}+\mathcal{O}(N^{-1}), \tag{2.14}$$

with $e_{ph}=e_p-e_h$ where

$$e_p=\langle\Psi_\mathbf{o}|\alpha_p H'\alpha_p^\dagger|\Psi_\mathbf{o}\rangle=t(p)+u(p),$$

$$e_h=-\langle\Psi_\mathbf{o}|\alpha_h^\dagger H'\alpha_h|\Psi_\mathbf{o}\rangle=t(h)+u(h) \tag{2.15}$$

and $u(p)$ is an average field that can be expressed in terms of the compound diagrammatic quantities of FHNC theory.

For the off-diagonal elements $O_{\mathbf{m},\mathbf{n}}$ of an operator O (specifically the Hamiltonian, the unit, density, and current operator) we sort the quantum numbers m_i and n_i such that $|\Psi_\mathbf{m}\rangle$ is mapped onto $|\Psi_\mathbf{n}\rangle$ by

$$|\Psi_\mathbf{m}\rangle=\alpha_{m_1}^\dagger\alpha_{m_2}^\dagger\ldots\alpha_{m_d}^\dagger\alpha_{n_d}\ldots\alpha_{n_2}\alpha_{n_1}|\Psi_\mathbf{n}\rangle. \tag{2.16}$$

From this we recognize that, to leading order in N, any $O_{\mathbf{m},\mathbf{n}}$ depends only on the *difference* between the states $|\Psi_\mathbf{m}\rangle$ and $|\Psi_\mathbf{n}\rangle$ and *not* on the states as a whole. Consequently, $O_{\mathbf{m},\mathbf{n}}$ can be written as matrix element of a d-body operator

$$O_{\mathbf{m},\mathbf{n}} \equiv \langle m_1 m_2, \ldots, m_d | \mathcal{O}(1,2,\ldots,d) | n_1 n_2, \ldots, n_d \rangle_a. \tag{2.17}$$

(The index a indicates antisymmetrization.) According to Eq. (2.17), $W_{\mathbf{m},\mathbf{n}}$ and $N_{\mathbf{m},\mathbf{n}}$ define d-particle operators $\mathcal{N}$ and $\mathcal{W}$, e.g.,

$$\begin{aligned} N_{\mathbf{m},\mathbf{o}} &\equiv N_{p_1 p_2, \ldots, p_d h_1 h_2, \ldots, h_d, 0} \\ &\equiv \langle p_1 p_2, \ldots, p_d | \mathcal{N}(1,2,\ldots,d) | h_1 h_2, \ldots, h_d \rangle_a, \end{aligned}$$

$$\begin{aligned} W_{\mathbf{m},\mathbf{o}} &\equiv W_{p_1 p_2, \ldots, p_d h_1 h_2, \ldots, h_d, 0} \\ &\equiv \langle p_1 p_2, \ldots, p_d | \mathcal{W}(1,2,\ldots,d) | h_1 h_2, \ldots, h_d \rangle_a. \end{aligned} \tag{2.18}$$

Diagrammatic representations of $\mathcal{N}(1,2,\ldots,d)$ and $\mathcal{W}(1,2,\ldots,d)$ have the same topology.[31] In homogeneous systems, the continuous parts of the p_i, h_i are wave numbers $\mathbf{p}_i, \mathbf{h}_i$; we abbreviate their difference as $\mathbf{q}_i$. The highest occupied momentum is $\hbar k_F$.

An important consideration is, for our purposes, the connection between CBF matrix elements, the static structure function, and the optimization conditions for the ground state. The static structure function $S(q) = \frac{1}{N} \langle \Psi_\mathbf{o} | \hat{\rho}_\mathbf{q} \hat{\rho}_{-\mathbf{q}} | \Psi_\mathbf{o} \rangle$ is routinely obtained in ground-state calculations; for some systems it is also available from experiments. We can also write $S(q)$ as the weighted average of the matrix elements Eq. (2.18),

$$S(q) = S_F(q) + \frac{1}{N} \sum_{hh'} z_{pp'hh'} N_{pp'hh',0}, \tag{2.19}$$

where $S_F(q)$ is the static structure function of noninteracting fermions.

Similarly, the optimization conditions Eq. (2.5) for the pair-correlation function can, in momentum space, be written in terms of off-diagonal matrix elements of the Hamiltonian

$$\begin{aligned} 0 &= \frac{\delta E}{\delta \tilde{u}_2(\mathbf{q},\mathbf{q}')} = \frac{\langle \Phi_\mathbf{o} | F^\dagger H' F [\hat{\rho}_\mathbf{q} \hat{\rho}_{\mathbf{q}'} - \hat{\rho}_{\mathbf{q}+\mathbf{q}'}] | \Phi_\mathbf{o} \rangle}{\langle \Phi_\mathbf{o} | F^\dagger F | \Phi_\mathbf{o} \rangle} \\ &= \sum_{hh'} \frac{\langle \Phi_\mathbf{o} | F^\dagger H' F | a^\dagger_{p'} a^\dagger_p a_h a_{h'} \Phi_\mathbf{o} \rangle}{\langle \Phi_\mathbf{o} | F^\dagger F | \Phi_\mathbf{o} \rangle} = \sum_{hh'} z_{pp'hh'} H'_{pp'hh',0}, \end{aligned} \tag{2.20}$$

i.e., the weighted average of the off-diagonal matrix elements $H'_{0,pp'hh'}$ vanishes for optimized pair correlations. Both features will provide rules for systematic and consistent approximation schemes for the operators $\mathcal{N}(1,2,\ldots,d)$ and $\mathcal{W}(1,2,\ldots,d)$.

III. EQUATIONS OF MOTION

A. Excitation operator and action principle

To formulate a theory of excited states for strongly interacting fermions we generalize the ansatz Eqs. (2.2) and (2.3) in analogy to the pair-fluctuations theory for strongly interacting bosons.[6,7,12,14–17] We restrict ourselves here to uniform systems. The system is subjected to a small external perturbation

$$H_{\text{ext}}(t) \equiv \int d^3 r h_{\text{ext}}(\mathbf{r};t) \hat{\rho}(\mathbf{r}), \tag{3.1}$$

where $\hat{\rho}(\mathbf{r})$ is the density operator. The correlated wave function for the perturbed state is chosen to be

$$\begin{aligned} |\Psi(t)\rangle &= \exp[-iH_{\mathbf{o},\mathbf{o}} t/\hbar] |\Psi_0(t)\rangle, \\ |\Psi_0(t)\rangle &= \frac{1}{I^{1/2}(t)} \exp\left[\frac{1}{2} U(t)\right] |\Psi_\mathbf{o}\rangle, \\ I(t) &= \langle \Psi_\mathbf{o} | \exp\left[\frac{1}{2} U^\dagger(t)\right] \exp\left[\frac{1}{2} U(t)\right] | \Psi_\mathbf{o} \rangle \end{aligned} \tag{3.2}$$

with the excitation operator

$$\begin{aligned} U(t) &\equiv \sum_{ph} \delta u^{(1)}_{ph}(t) \alpha^\dagger_p \alpha_h + \frac{1}{2} \sum_{pp'hh'} \delta u^{(2)}_{pp'hh'}(t) \alpha^\dagger_p \alpha^\dagger_{p'} \alpha_{h'} \alpha_h \\ &\equiv U_1(t) + U_2(t). \end{aligned} \tag{3.3}$$

The particle-hole amplitudes $\delta u^{(1)}_{ph}(t)$ and $\delta u^{(2)}_{pp'hh'}(t)$ are determined by the stationarity principle for the action

$$\mathcal{S}[\delta u^{(1)}, \delta u^{(1)*}, \delta u^{(2)}, \delta u^{(2)*}] = \int dt \mathcal{L}(t) \tag{3.4}$$

with the Lagrangian[1,2,4,5]

$$\begin{aligned} \mathcal{L}(t) &= \langle \Psi(t) | H + H_{\text{ext}}(t) - i\hbar \frac{\partial}{\partial t} | \Psi(t) \rangle \\ &= \langle \Psi_0(t) | H' + H_{\text{ext}}(t) - i\hbar \frac{\partial}{\partial t} | \Psi_0(t) \rangle. \end{aligned} \tag{3.5}$$

A "boson" version of the theory is recovered when the particle-hole amplitudes $\delta u^{(1)}_{ph}(t)$ and $\delta u^{(2)}_{pp'hh'}(t)$ are restricted to *local* functions that depend only on the momentum transfers $\mathbf{q}^{(\prime)} = \mathbf{p}^{(\prime)} - \mathbf{h}^{(\prime)}$.

B. Brillouin conditions

To derive linear equations of motion, the Lagrangian (3.5) must be expanded to second order in the excitation operator $U(t)$. For the procedure to be meaningful, one should require that the first-order terms vanish. This is, in principle, a necessary condition, however, in practice it is not always possible to satisfy it rigorously.

The first variation in the energy with respect to $\delta u^{(1)}_{ph}(t)$ and $\delta u^{(1)*}_{ph}(t)$ is

$$\left. \frac{\delta \langle \Psi(t) | H' | \Psi(t) \rangle}{\delta [\delta u^{(1)}_{ph}(t)]} \right|_{\delta u^{(1)}_{ph}(t) = \delta u^{(2)}_{pp'hh'}(t) = 0} = H'_{0,ph} \tag{3.6}$$

and its complex conjugate. This term vanishes in the homogeneous liquid due to momentum conservation.

The variation with respect to $\delta u^{(2)}_{pp'hh'}(t)$ leads to a similar condition

$$\left.\frac{\delta\langle\Psi(t)|H'|\Psi(t)\rangle}{\delta[\,\delta u^{(2)}_{pp'hh'}(t)]}\right|_{\delta u^{(1)}_{ph}(t)=\delta u^{(2)}_{pp'hh'}(t)=0} = H'_{0,pp'hh'} = 0 \tag{3.7}$$

and its complex conjugate. This condition is not rigorously satisfied by a Jastrow-Feenberg ground state. Recall, however, that the optimization condition Eq. (2.5) for pair correlations can be written in terms of off-diagonal matrix elements of H' in the form Eq. (2.20). If the correlation operator F is chosen optimally, i.e., satisfying Eq. (2.5) for all n, the weighted averages of $H_{\mathbf{o},\mathbf{n}}$ vanish. This shows precisely what an optimized ground state does. The Jastrow-correlation function does not have enough flexibility to guarantee the Brillouin condition Eq. (3.7) because $H'_{0,pp'hh'}$ depends nontrivially on four momenta whereas the two-body Jastrow-Feenberg function depends only on the momentum transfer. Optimization has the effect that the Brillouin conditions are satisfied in the Fermi-sea average.

To make progress we must assume that in the Lagrangian terms that are linear in the pair fluctuations are sufficiently small and can be omitted. Likewise, we also shall assume that the ground-state correlation function Eq. (2.3) is well enough optimized such that three- and four-body Brillouin conditions are satisfied. In momentum space, these are

$$\langle\Psi_0|H'\rho_{\mathbf{q}_1}\cdots\rho_{\mathbf{q}_n}|\Psi_0\rangle = 0. \tag{3.8}$$

C. Transition density

The quantity of primary interest is the linear density fluctuation induced by the external field $H_{\mathrm{ext}}(t)$. We regard this density as a *complex* quantity; it is understood that the physical density fluctuation is its real part. Assuming the excitation operator Eq. (3.3), it is

$$\begin{aligned}\delta\rho(\mathbf{r};t) &= \sum_{ph}\langle\Psi_{\mathbf{o}}|\hat{\rho}(\mathbf{r})-\rho|\Psi_{ph}\rangle\,\delta u^{(1)}_{ph}(t)\\ &\quad+\frac{1}{2}\sum_{pp'hh'}\langle\Psi_{\mathbf{o}}|\hat{\rho}(\mathbf{r})-\rho|\Psi_{pp'h'h}\rangle\,\delta u^{(2)}_{pp'hh'}(t)\\ &\equiv\sum_{ph}\rho_{0,ph}(\mathbf{r})\,\delta u^{(1)}_{ph}(t)\\ &\quad+\frac{1}{2}\sum_{pp'hh'}\rho_{0,pp'hh'}(\mathbf{r})\,\delta u^{(2)}_{pp'hh'}(t).\end{aligned} \tag{3.9}$$

The matrix elements of the density with respect to the correlated states can also be written as linear combinations of the matrix elements $\rho^{\mathrm{F}}_{0,ph}(\mathbf{r})$ with respect to uncorrelated states, and one-, two-, and three-body matrix elements of the unit operator. For the sake of discussion, let us briefly neglect the pair amplitudes. Since the density operator is local, we can commute $\hat{\rho}(\mathbf{r})$ to the right or to the left of the correlation operator F. The form obtained by commuting $\hat{\rho}(\mathbf{r})$ to the left is

$$\begin{aligned}\rho_{0,ph}(\mathbf{r}) &= \sum_{p'h'}\tilde{\rho}^{\mathrm{F}}_{0,p'h'}(\mathbf{r})M_{p'h',ph}\\ &= \tilde{\rho}^{\mathrm{F}}_{0,ph}(\mathbf{r})+\sum_{p'h'}\tilde{\rho}^{\mathrm{F}}_{0,p'h'}(\mathbf{r})N_{p'h',ph},\end{aligned} \tag{3.10}$$

where $\tilde{\rho}^{F}_{0,ph}(\mathbf{r})\equiv z_{ph}\langle\Phi_{\mathbf{o}}|\hat{\rho}(\mathbf{r})-\rho|a^{\dagger}_p a_h\Phi_{\mathbf{o}}\rangle\equiv z_{ph}\langle h|\,\delta\hat{\rho}(\mathbf{r})|p\rangle$ are, apart from the normalization factors z_{ph}, the matrix elements of the density operator in a noninteracting system.

The second form is obtained by commuting $\hat{\rho}(\mathbf{r})$ to the right of F

$$\rho_{0,ph}(\mathbf{r}) = \frac{1}{z^2_{ph}}\tilde{\rho}^{\mathrm{F}}_{0,ph}(\mathbf{r})+\sum_{p'h'}N_{0,pp'hh'}\tilde{\rho}^{\mathrm{F}}_{p'h',0}(\mathbf{r}). \tag{3.11}$$

These two seemingly different expressions are identical, the different analytic forms appear only because the second quantized formulation hides the fact that the density operator is local. We will see below that both forms are useful.

Including pair fluctuations, the fluctuating density Eq. (3.9) can generally be written as

$$\begin{aligned}\delta\rho(\mathbf{r};t) = \sum_{ph}\tilde{\rho}^{\mathrm{F}}_{0,ph}(\mathbf{r})\Bigg[&\sum_{p'h'}M_{ph,p'h'}\,\delta u^{(1)}_{p'h'}(t)\\ &+\frac{1}{2}\sum_{p'p''h'h''}M_{ph,p'p''h'h''}\,\delta u^{(2)}_{p'p''h'h''}(t)\Bigg].\end{aligned} \tag{3.12}$$

A key step that simplifies the structure of the equations of motion significantly is to introduce a new one-body function. In analogy to the boson theory,[7] we define new particle-hole amplitudes $\delta v^{(1)}_{ph}(t)$ through

$$\delta\rho(\mathbf{r};t)\equiv\sum_{ph}\rho_{0,ph}(\mathbf{r})\,\delta v^{(1)}_{ph}(t) \tag{3.13}$$

such that

$$\delta\rho(\mathbf{r};t) = \sum_{php'h'}\tilde{\rho}^{\mathrm{F}}_{0,ph}(\mathbf{r})M_{ph,p'h'}\,\delta v^{(1)}_{p'h'}(t). \tag{3.14}$$

This implies

$$\begin{aligned}\sum_{p'h'}M_{ph,p'h'}\,\delta v^{(1)}_{p'h'}(t) &= \sum_{p'h'}M_{ph,p'h'}\,\delta u^{(1)}_{p'h'}(t)\\ &\quad+\frac{1}{2}\sum_{p'p''h'h''}M_{ph,p'p''h'h''}\,\delta u^{(2)}_{p'p''h'h''}(t).\end{aligned} \tag{3.15}$$

Defining $M^{(\mathrm{I})}_{ph,p'p''h'h''}$ via

$$M_{ph,p'p''h'h''}\equiv\sum_{p_1h_1}M_{ph,p_1h_1}M^{(\mathrm{I})}_{p_1h_1,p'p''h'h''} \tag{3.16}$$

we can formally solve for $\delta v^{(1)}_{ph}(t)$

$$\delta v^{(1)}_{ph}(t) = \delta u^{(1)}_{ph}(t) + \frac{1}{2}\sum_{p'p''h'h''} M^{(\mathrm{I})}_{ph,p'p''h'h''}\delta u^{(2)}_{p'p''h'h''}(t). \tag{3.17}$$

For this operation, the inverse of $M_{ph,p'h'}$ seems to be needed. As its calculation is not immediately obvious, we hasten to note that $M^{(\mathrm{I})}_{ph,p'p''h'h''}$ is, in terms of Jastrow-Feenberg diagrams,[31] a *proper subset* of the diagrams contributing to $M_{ph,p'p''h'h''}$. We will discuss the diagrammatic analysis of $\rho_{0,ph}(\mathbf{r})$ in Appendix B 1. The diagrammatic construction of $M^{(\mathrm{I})}_{ph,p'p''h'h''}$ in the spirit of Eq. (3.16) is carried out in Appendix B 2.

D. Lagrangian

We split Lagrangian (3.5) as $\mathcal{L}(t)=\mathcal{L}_{\mathrm{ext}}(t)+\mathcal{L}_{\mathrm{t}}(t)+\mathcal{L}_{\mathrm{int}}(t)$ with

$$\mathcal{L}_{\mathrm{ext}}(t) = \langle\Psi_0(t)|H_{\mathrm{ext}}|\Psi_0(t)\rangle, \tag{3.18}$$

$$\mathcal{L}_{\mathrm{t}}(t) = \langle\Psi_0(t)|-i\hbar\frac{\partial}{\partial t}|\Psi_0(t)\rangle, \tag{3.19}$$

$$\mathcal{L}_{\mathrm{int}}(t) = \langle\Psi_0(t)|H'|\Psi_0(t)\rangle. \tag{3.20}$$

$\mathcal{L}_{\mathrm{ext}}(t)$ is obtained directly from the transition density

$$\begin{aligned}\mathcal{L}_{\mathrm{ext}}(t) &= \int d^3r h_{\mathrm{ext}}(\mathbf{r};t)\delta\rho(\mathbf{r};t)\\ &= \int d^3r h_{\mathrm{ext}}(\mathbf{r};t)\Re e\left[\sum_{ph}\rho_{0,ph}(\mathbf{r})\delta u^{(1)}_{ph}(t)\right.\\ &\quad\left.+\frac{1}{2}\sum_{pp'hh'}\rho_{0,pp'hh'}(\mathbf{r})\delta u^{(2)}_{pp'hh'}(t)\right]\\ &= \Re e\sum_{ph}\int d^3r h_{\mathrm{ext}}(\mathbf{r};t)\rho_{0,ph}(\mathbf{r})\delta v^{(1)}_{ph}(t).\end{aligned} \tag{3.21}$$

The time-derivative term $\mathcal{L}_t(t)$ is, to second order in the fluctuations,

$$\begin{aligned}\mathcal{L}_{\mathrm{t}}(t) &= \frac{\hbar}{2\langle\Psi_0(t)|\Psi_0(t)\rangle}\Im\mathrm{m}\sum\left[\delta\dot{u}^{(1)}_{ph}(t)\langle\psi(t)|\alpha^\dagger_p\alpha_h\psi(t)\rangle\right.\\ &\quad\left.+\frac{1}{2}\sum\delta\dot{u}^{(2)}_{pp'hh'}(t)\langle\Psi_0(t)|\alpha^\dagger_p\alpha^\dagger_{p'}\alpha_{h'}\alpha_h\Psi_0(t)\rangle\right]\\ &= \frac{\hbar}{4}\Im\mathrm{m}\left[\sum\delta u^{(1)*}_{ph}(t)M_{ph,p'h'}\delta\dot{u}^{(1)}_{p'h'}(t)\right.\\ &\quad+\frac{1}{2}\sum\delta u^{(1)*}_{ph}(t)M_{ph,p'p''h'h''}\delta\dot{u}^{(2)}_{p'p''h'h''}(t)\\ &\quad+\frac{1}{2}\sum\delta u^{(2)*}_{pp'hh'}(t)M_{pp'hh',p''h''}\delta\dot{u}^{(1)}_{p''h''}(t)\\ &\quad\left.+\frac{1}{4}\sum\delta u^{(2)*}_{pp'hh'}(t)M_{pp'hh',p''p'''h''h'''}\delta\dot{u}^{(2)}_{p''p'''h''h'''}(t)\right].\end{aligned} \tag{3.22}$$

Introducing the new amplitudes $\delta v^{(1)}_{ph}(t)$ defined in Eq. (3.13) eliminates the terms that couple the one- and the two-body amplitudes

$$\begin{aligned}\mathcal{L}_{\mathrm{t}}(t) &= \frac{\hbar}{4}\Im\mathrm{m}\left[\sum\delta v^{(1)*}_{ph}(t)M_{ph,p'h'}\delta\dot{v}^{(1)}_{p'h'}(t)\right.\\ &\quad\left.+\frac{1}{4}\sum\delta u^{(2)*}_{pp'hh'}(t)M^{(\mathrm{I})}_{pp'hh',p''p'''h''h'''}\delta\dot{u}^{(2)}_{p''p'''h''h'''}(t)\right],\end{aligned} \tag{3.23}$$

where

$$\begin{aligned}M^{(\mathrm{I})}_{pp'hh',p''p'''h''h'''} &= M_{pp'hh',p''p'''h''h'''}\\ &\quad-\sum_{p_1p_2h_1h_2}M^{(\mathrm{I})}_{pp'hh',p_1h_1}M_{p_1h_1,p_2h_2}\\ &\quad\times M^{(\mathrm{I})}_{p_2h_2,p''p'''h''h'''}.\end{aligned} \tag{3.24}$$

The second term in Eq. (3.24) cancels, in a diagrammatic expansion, some terms from the first one (cf. Appendix B 1). From Eqs. (3.21) and (3.23), the advantage of introducing the new particle-hole amplitudes $\delta v^{(1)}_{ph}(t)$ becomes obvious.

The contributions to the interaction term are classified according to the involved n-body fluctuations U_n as defined in Eq. (3.3),

$$\mathcal{L}_{\mathrm{int}}(t) = \mathcal{L}^{(11)}_{\mathrm{int}}(t) + \mathcal{L}^{(12)}_{\mathrm{int}}(t) + \mathcal{L}^{(22)}_{\mathrm{int}}(t) \tag{3.25}$$

with

$$\begin{aligned}\mathcal{L}^{(11)}_{\mathrm{int}}(t) &= \frac{1}{8}\langle\Psi_{\mathbf{o}}|[U^\dagger_1(t)U^\dagger_1(t)H' + 2U^\dagger_1(t)H'U_1(t)\\ &\quad + H'U_1(t)U_1(t)]|\Psi_{\mathbf{o}}\rangle,\\ \mathcal{L}^{(12)}_{\mathrm{int}}(t) &= \frac{1}{4}\langle\Psi_{\mathbf{o}}|[U^\dagger_1(t)U^\dagger_2(t)H' + U^\dagger_1(t)H'U_2(t)\\ &\quad + U^\dagger_2(t)H'U_1(t) + H'U_1(t)U_2(t)]|\Psi_{\mathbf{o}}\rangle,\\ \mathcal{L}^{(22)}_{\mathrm{int}}(t) &= \frac{1}{8}\langle\Psi_{\mathbf{o}}|[U^\dagger_2(t)U^\dagger_2(t)H' + 2U^\dagger_2(t)H'U_2(t)\\ &\quad + H'U_2(t)U_2(t)]|\Psi_{\mathbf{o}}\rangle.\end{aligned} \tag{3.26}$$

If the Brillouin conditions in Eqs. (3.6) and (3.7) as well as their generalizations to higher order fluctuations were satisfied exactly, all contributions to $\mathcal{L}^{(ij)}_{\mathrm{int}}(t)$ containing $U^\dagger_i(t)U^\dagger_j(t)$ and $U_i(t)U_j(t)$ would be zero. For fermions with optimized Jastrow-Feenberg wave functions it is only true in the averaged sense Eq. (2.20). These terms are nevertheless expected to be small in $\mathcal{L}^{(22)}_{\mathrm{int}}(t)$ since neglecting these terms is equivalent to negligible four-body correlations. Such a simplifying assumption is not necessary in $\mathcal{L}^{(12)}_{\mathrm{int}}(t)$ and $\mathcal{L}^{(11)}_{\mathrm{int}}(t)$ although we will see that the terms containing $U_1(t)U_2(t)$ and $U^\dagger_1(t)U^\dagger_2(t)$ in $\mathcal{L}^{(12)}_{\mathrm{int}}(t)$ are indeed negligible. We keep these terms for the time being since it will turn out that their omission will suggest, for consistency reasons, further simplifications.

The next step is to express the interaction term Eq. (3.26) in terms of the CBF matrix elements introduced in Sec. II B. In the following it is understood that we sum over all quantum numbers when no summation subscripts are spelled out.

$$\mathcal{L}_{\rm int}^{(11)}(t) = \frac{1}{8}\sum \delta u_{ph}^{(1)*}(t)\,\delta u_{p'h'}^{(1)*}(t) H'_{pp'hh',0} + \text{c.c.} + \frac{1}{4}\sum \delta u_{ph}^{(1)*}(t) H'_{ph,p'h'}\,\delta u_{p'h'}^{(1)}(t), \tag{3.27}$$

$$\mathcal{L}_{\rm int}^{(12)}(t) = \frac{1}{8}\sum \delta u_{ph}^{(1)*}(t)\,\delta u_{p'p''h'h''}^{(2)*}(t) H'_{pp'p''hh'h'',0} + \text{c.c.} + \frac{1}{8}\sum \delta u_{ph}^{(1)*}(t) H'_{ph,p'p''h'h''}\delta u_{p'p''h'h''}^{(2)}(t) + \text{c.c.}, \tag{3.28}$$

$$\mathcal{L}_{\rm int}^{(22)}(t) = \frac{1}{32}\sum \delta u_{pp'hh'}^{(2)*}(t)\,\delta u_{p''p'''h''h'''}^{(2)*}(t) H'_{pp'p''p'''hh'h''h''',0} + \text{c.c.} + \frac{1}{16}\sum \delta u_{pp'hh'}^{(2)*}(t) H'_{pp'hh',p''p'''h''h'''}\delta u_{p''p'''h''h'''}^{(2)}(t). \tag{3.29}$$

Substituting $\delta v_{ph}^{(1)}(t)$ for $\delta u_{ph}^{(1)}(t)$ leads to new coefficient functions in the interaction part of the Lagrangian

$$\mathcal{L}_{\rm int}(t) = \mathcal{L}_{\rm int}^{\prime(11)}(t) + \mathcal{L}_{\rm int}^{\prime(12)}(t) + \mathcal{L}_{\rm int}^{\prime(22)}(t) \tag{3.30}$$

with

$$\mathcal{L}_{\rm int}^{\prime(11)}(t) = \frac{1}{8}\sum \delta v_{ph}^{(1)*}(t)\,\delta v_{p'h'}^{(1)*}(t) H'_{pp'hh',0} + \text{c.c.} + \frac{1}{4}\sum \delta v_{ph}^{(1)*}(t) H'_{ph,p'h'}\,\delta v_{p'h'}^{(1)}(t), \tag{3.31}$$

$$\mathcal{L}_{\rm int}^{\prime(12)}(t) = \frac{1}{8}\sum \delta v_{ph}^{(1)*}(t)\,\delta u_{p'p''h'h''}^{(2)*}(t) K_{p'p''h'h'',0}^{(ph)} + \text{c.c.} + \frac{1}{8}\sum \delta v_{ph}^{(1)*}(t) K_{ph,p'p''h'h''}\,\delta u_{p'p''h'h''}^{(2)}(t) + \text{c.c.} \tag{3.32}$$

$$\mathcal{L}_{\rm int}^{\prime(22)}(t) = \frac{1}{32}\sum \delta u_{pp'hh'}^{(2)*}(t)\,\delta u_{p''p'''h''h'''}^{(2)*}(t) K_{p''p'''h''h''',0}^{(pp'hh')} + \text{c.c.} + \frac{1}{16}\sum \delta u_{pp'hh'}^{(2)*}(t) K_{pp'hh',p''p'''h''h'''}\,\delta u_{p''p'''h''h'''}^{(2)}(t). \tag{3.33}$$

The new coefficients $K_{\mathbf{m},\mathbf{n}}$ are

$$K_{ph,p'p''h'h''} \equiv H'_{ph,p'p''h'h''} - \sum_{p_1h_1} H'_{ph,p_1h_1} M^{(\rm I)}_{p_1h_1,p'p''h'h''}, \tag{3.34}$$

$$K_{p'p''h'h'',0}^{(ph)} \equiv H'_{pp'p''hh'h'',0} - \sum_{p_1h_1} H'_{php_1h_1,0} M^{(\rm I)}_{p'p''h'h'',p_1h_1}, \tag{3.35}$$

$$\begin{aligned} K_{pp'hh',p''p'''h''h'''} \equiv{}& H'_{pp'hh',p''p'''h''h'''} \\ &- \sum_{p_1h_1} (M^{(\rm I)}_{pp'hh',p_1h_1} H'_{p_1h_1,p''p'''h''h'''} \\ &+ H'_{pp'hh',p_1h_1} M^{(\rm I)}_{p_1h_1,p''p'''h''h'''}) \\ &+ \sum_{p_1h_1p_2h_2} M^{(\rm I)}_{pp'hh',p_1h_1} H'_{p_1h_1,p_2h_2} \\ &\times M^{(\rm I)}_{p_2h_2,p''p'''h''h'''}, \end{aligned} \tag{3.36}$$

and an analogous term for $K_{p''p'''h''h''',0}^{(pp'hh')}$.

E. Equations of motion

With the sole approximation to neglect the terms proportional to $U_2(t)U_2(t)$ and $U_2^\dagger(t)U_2^\dagger(t)$, the Euler equations become

$$\sum_{p'h'}\left[i\hbar M_{ph,p'h'}\frac{\partial}{\partial t} - H'_{ph,p'h'}\right]\delta v_{p'h'}^{(1)}(t) - \sum_{p'h'} H'_{pp'hh',0}\delta v_{p'h'}^{(1)*}(t) - \frac{1}{2}\sum_{p'p''h'h''}[K_{ph,p'p''h'h''}\delta u_{p'p''h'h''}^{(2)}(t) + K_{p'p''h'h'',0}^{(ph)}\delta u_{p'p''h'h''}^{(2)*}(t)] = 2\int d^3r\rho_{ph,0}(\mathbf{r})h_{\rm ext}(\mathbf{r};t), \tag{3.37}$$

$$\frac{1}{2}\sum_{p''p'''h''h'''}\left[i\hbar M^{(\rm I)}_{pp'hh',p''p'''h''h'''}\frac{\partial}{\partial t} - K_{pp'hh',p''p'''h''h'''}\right]\delta u_{p''p'''h''h'''}^{(2)}(t) - \sum_{p''p'''h''h'''}[K_{pp'hh',p''h''}\delta v_{p''h''}^{(1)}(t) + K_{pp'hh',0}^{(p''h'')}\delta v_{p''h''}^{(1)*}(t)] = 0. \tag{3.38}$$

The time dependence of the external field can be assumed to be harmonic with an infinitesimal turn-on component that determines the sign of the imaginary part

$$h_{\text{ext}}(\mathbf{r};t) = h_{\text{ext}}(\mathbf{r};\omega)[e^{i\omega t} + e^{-i\omega t}]e^{\eta t/\hbar}. \tag{3.39}$$

This imposes the time dependence

$$\delta v^{(1)}_{ph}(t) = \delta v^{(1+)}_{ph}(\omega)e^{-i(\omega+i\eta/\hbar)t} + [\delta v^{(1-)}_{ph}(\omega)e^{-i(\omega+i\eta/\hbar)t}]^*,$$

$$\delta u^{(2)}_{pp'hh'}(t) = \delta u^{(2+)}_{pp'hh'}(\omega)e^{-i(\omega+i\eta/\hbar)t} + [\delta u^{(2-)}_{pp'hh'}(\omega)e^{-i(\omega+i\eta/\hbar)t}]^*. \tag{3.40}$$

Defining

$$E_{pp'hh',p''p'''h''h'''}(\omega) \equiv (\hbar\omega + i\eta)M^{(\mathrm{I})}_{pp'hh',p''p'''h''h'''} - K_{pp'hh',p''p'''h''h'''} \tag{3.41}$$

the equations of motion for the pair fluctuations are

$$\frac{1}{2}\sum_{p''p'''h''h'''} E_{pp'hh',p''p'''h''h'''}(\omega)\,\delta u^{(2+)}_{p''p'''h''h'''}(\omega) = \sum_{p''h''}[K_{pp'hh',p''h''}\delta v^{(1+)}_{p''h''}(\omega) + K^{(p''h'')}_{pp'hh',0}\delta v^{(1-)}_{p''h''}(\omega)],$$

$$\frac{1}{2}\sum_{p''p'''h''h'''} E^*_{pp'hh',p''p'''h''h'''}(-\omega)\,\delta u^{(2-)}_{p''p'''h''h'''}(\omega) = \sum_{p''h''}[K^*_{pp'hh',p''h''}\delta v^{(1-)}_{p''h''}(\omega) + K^{(p''h'')*}_{pp'hh',0}\delta v^{(1+)}_{p''h''}(\omega)]. \tag{3.42}$$

All pair quantities are symmetric under the interchange of the involved pair variables, e.g., $(pp',hh') \leftrightarrow (p'p,h'h)$. We can utilize this feature to replace the fully symmetric $E_{pp'hh',p''p'''h''h'''}(\omega)$ by an asymmetric form, e.g., Eq. (C1), which removes the factor 1/2 in Eq. (3.42).

The pair Eqs. (3.42) are now solved for the $\delta u^{(2\pm)}_{pp'hh'}(\omega)$ and the solutions are inserted into the one-body equation. The latter retains the structure of a TDHF equation but with the matrix elements of H' supplemented by frequency-dependent terms. We adapt the definition of $W_{\mathbf{m},\mathbf{n}}$ in Eq. (2.11) by adding these corrections

$$W_{ph,p'h'}(\omega) = W_{ph,p'h'} + \sum_{p_ih_ip'_ih'_i} K_{ph,p_1p_2h_1h_2}E^{-1}_{p_1p_2h_1h_2,p'_1p'_2h'_1h'_2}(\omega)K_{p'_1p'_2h'_1h'_2,p'h'} + \sum_{p_ih_ip'_ih'_i} K^{(ph)}_{p_1p_2h_1h_2,0}E^{*-1}_{p_1p_2h_1h_2,p'_1p'_2h'_1h'_2}(-\omega)K^{(p'h')*}_{p'_1p'_2h'_1h'_2,0}, \tag{3.43}$$

$$W_{pp'hh',0}(\omega) = W_{pp'hh',0} + \sum_{p_ih_ip'_ih'_i} K_{ph,p_1p_2h_1h_2}E^{-1}_{p_1p_2h_1h_2,p'_1p'_2h'_1h'_2}(\omega)K^{(p'h')}_{p'_1p'_2h'_1h'_2,0} + \sum_{p_ih_ip'_ih'_i} K^{(ph)}_{p_1p_2h_1h_2,0}E^{*-1}_{p_1p_2h_1h_2,p'_1p'_2h'_1h'_2}(-\omega)K^*_{p'_1p'_2h'_1h'_2,p'h'}. \tag{3.44}$$

This TDHF form results also if the terms containing $U_2(t)U_2(t)$ are retained but the expressions for the dynamic parts of the W matrices become lengthier.

The equations of motion for the particle-hole amplitudes are then

$$2\int d^3r h_{\text{ext}}(\mathbf{r};\omega)\rho_{0,ph}(\mathbf{r}) = \sum_{p'h'}[(\hbar\omega + i\eta)M_{ph,p'h'} - \delta_{p,p'}\delta_{h,h'}e_{ph}]v^{(1+)}_{p'h'}(\omega) - \sum_{p'h'}\left[W_{ph,p'h'}(\omega) + \frac{1}{2}(e_{ph}+e_{p'h'})N_{ph,p'h'}\right]\delta v^{(1+)}_{p'h'}(\omega)$$
$$- \sum_{p'h'}\left[W_{pp'hh',0}(\omega) + \frac{1}{2}(e_{ph}+e_{p'h'})N_{pp'hh',0}\right]\delta v^{(1-)}_{p'h'}(\omega). \tag{3.45}$$

F. Supermatrix representation

We can now carry out exactly the same manipulations as in previous work[5] and reduce this Eq. (3.45) to the form of TDHF equations with energy-dependent effective interactions. Equations (3.10) and (3.11) express the density in terms of CBF matrix elements in two different forms. For the present purpose, it is convenient to use these two representations symmetrically,

$$\delta\rho_{0,ph}(\mathbf{r}) = \frac{1}{2}\left[1 + \frac{1}{z^2_{ph}}\right]\tilde{\rho}^{\mathrm{F}}_{0,ph}(\mathbf{r}) + \frac{1}{2}\sum_{p'h'}[\tilde{\rho}^{\mathrm{F}}_{0,p'h'}N_{p'h',ph} + \tilde{\rho}^{\mathrm{F}*}_{0,p'h'}(\mathbf{r})N_{0,pp'hh'}]. \tag{3.46}$$

Using Eqs. (3.13) and (3.40), the density fluctuations can then be written as

$$\delta\rho(\mathbf{r};\omega) = \frac{1}{2}\sum_{ph}\left[\rho_{0,ph}(\mathbf{r})\,\delta v_{ph}^{(1+)}(\omega) + \rho_{0,ph}^{*}(\mathbf{r})\,\delta v_{ph}^{(1-)}(\omega)\right]$$

$$\equiv \frac{1}{2}\sum_{ph}\left[\tilde{\rho}_{0,ph}^{\mathrm{F}}(\mathbf{r})\,\delta c_{ph}^{(1+)}(\omega) + \tilde{\rho}_{0,ph}^{\mathrm{F}*}(\mathbf{r})\,\delta c_{ph}^{(1-)}(\omega)\right], \tag{3.47}$$

[cf. Eq. (3.10) for the definition of $\tilde{\rho}_{0,ph}^{\mathrm{F}}(\mathbf{r})$]. This defines new amplitudes $\delta c_{ph}^{(1\pm)}(\omega)$. These relate, apart from the normalization factors, the observed density to the matrix elements of the density operator in the noninteracting system. The equations of motion can now be simplified by introducing a "supermatrix" notation. Particle-hole matrix elements together with their complex conjugate are combined into vectors, e.g.,

$$\tilde{\boldsymbol{\rho}}^{\mathrm{F}} \equiv \begin{pmatrix} \tilde{\rho}_{0,ph}^{\mathrm{F}} \\ \tilde{\rho}_{0,ph}^{F*} \end{pmatrix}; \quad \delta\mathbf{c} \equiv \begin{pmatrix} \delta c_{ph}^{(1+)} \\ \delta c_{ph}^{(1-)} \end{pmatrix} \tag{3.48}$$

(and analogously for $\delta v_{ph}^{(1\pm)}$). Equation (3.47) then simply reads

$$\delta\rho(\mathbf{r};\omega) = \frac{1}{2}\delta\mathbf{c}(\omega)\cdot\tilde{\boldsymbol{\rho}}^{\mathrm{F}}(\mathbf{r}). \tag{3.49}$$

The matrices

$$\mathbf{N} = \begin{pmatrix} N_{ph,p'h'} & N_{pp'hh',0} \\ N_{0,pp'hh'} & N_{p'h',ph} \end{pmatrix} \tag{3.50}$$

and

$$\mathbf{C} = \frac{1}{2}\begin{pmatrix} 1+\dfrac{1}{z_{ph}^{2}} & 0 \\ 0 & 1+\dfrac{1}{z_{ph}^{2}} \end{pmatrix}\delta_{p,p'}\delta_{h,h'} + \frac{1}{2}\mathbf{N} \tag{3.51}$$

relate the amplitudes

$$\delta\mathbf{c} = \mathbf{C}\cdot\delta\mathbf{v}. \tag{3.52}$$

In the driving term on the lhs of Eq. (3.45) we use $\rho_{0,ph} = (\mathbf{C}\cdot\tilde{\boldsymbol{\rho}}^{\mathrm{F}})_{0,ph}$ to obtain

$$2\int d^{3}r h_{\mathrm{ext}}(\mathbf{r};\omega)\rho_{0,ph}(\mathbf{r}) = 2\mathbf{C}\cdot\mathbf{h}^{\mathrm{ext}}, \tag{3.53}$$

where the vector $\mathbf{h}^{\mathrm{ext}}$ is built with the noninteracting states [cf. $\tilde{\rho}_{0,ph}^{\mathrm{F}}$ in Eq. (3.10)]

$$\tilde{h}_{0,ph}^{\mathrm{F}}(\omega) = z_{ph}\langle h|h_{\mathrm{ext}}(\mathbf{r};\omega)|p\rangle. \tag{3.54}$$

Defining the ω-dependent matrices

$$\boldsymbol{\Omega} = \begin{pmatrix} \hbar\omega + i\eta - e_{ph} & 0 \\ 0 & -(\hbar\omega + i\eta + e_{ph}) \end{pmatrix}\delta_{p,p'}\delta_{h,h'},$$

$$\mathbf{W} = \begin{pmatrix} W_{ph,p'h'}^{(+)}(\omega) & W_{pp'hh',0}^{(-)}(\omega) \\ W_{0,pp'hh'}^{(+)}(\omega) & W_{p'h',ph}^{(-)}(\omega) \end{pmatrix}, \tag{3.55}$$

the equations of motion assume supermatrix form[5]

$$\left[\boldsymbol{\Omega} + \frac{1}{2}\boldsymbol{\Omega}\mathbf{N} + \frac{1}{2}\mathbf{N}\boldsymbol{\Omega} - \mathbf{W}(\omega)\right]\delta\mathbf{v} = 2\mathbf{C}\mathbf{h}^{\mathrm{ext}}. \tag{3.56}$$

We now formally define a new, energy-dependent interaction matrix $\mathbf{V}_{\text{p-h}}(\omega)$ by

$$\left[\boldsymbol{\Omega} + \frac{1}{2}\boldsymbol{\Omega}\mathbf{N} + \frac{1}{2}\mathbf{N}\boldsymbol{\Omega} - \mathbf{W}\right] \equiv \mathbf{C}\cdot[\boldsymbol{\Omega} - \mathbf{V}_{\text{p-h}}(\omega)]\mathbf{C}. \tag{3.57}$$

Thus the response equations take the simple TDHF form

$$[\boldsymbol{\Omega} - \mathbf{V}_{\text{p-h}}(\omega)]\delta\mathbf{c} = 2\mathbf{h}^{\mathrm{ext}}. \tag{3.58}$$

With this, we have reformulated the theory for a strongly interacting system in the TDHF form Eq. (3.58) but with an energy-dependent effective interaction. Our derivation has led to a clear definition of this effective particle-hole interaction and to a prescription on how to calculate this from the underlying bare Hamiltonian.

The formal derivation appears to involve the calculation of the inverse of a huge matrix. The key point, however, is that the manipulation Eq. (3.57) can be carried out diagrammatically. Then it becomes obvious that many terms occurring in the combination of matrices in Eq. (3.56) are *not* part of $\mathbf{V}_{\text{p-h}}(\omega)$. Specifically, these are the chain diagrams in the direct channel.[5]

IV. DIAGRAMMATIC ANALYSIS AND LOCAL INTERACTIONS

A. General strategy

Generally, the nonlocal operators $\mathcal{N}(1,2)$ and $\mathcal{W}(1,2)$ in Eq. (2.18) consist of up to four-point functions. Cluster expansions and resummations have been carried out in Ref. 31 and led to reasonably compact representations in terms of the compound-diagrammmatic quantities of the FHNC summation method. Nevertheless, due to their nonlocality, it is difficult to deal with these quantities exactly. The simplest approximation for the operator is to keep just the local terms. These are given by the "direct-direct" correlation function $\Gamma_{\mathrm{dd}}(|\mathbf{r}_1-\mathbf{r}_2|)$ of FHNC theory. This approximation is adequate but not optimal.

On the other hand, summing $N_{0,pp'hh'}$ over the hole states, Eq. (2.19), relates $\mathcal{N}(1,2)$ to the static structure function. Accurate results are available for $S(q)$, either from simulations[33,34] or from the FHNC-EL summation technique.[28,35] An alternative strategy to deal with nonlocal operators is therefore to demand that these results are reproduced in whatever approximate form one chooses to use. In this sense, by *choosing* $\mathcal{N}(1,2)$ to be local, *naming* the corresponding function $\Gamma_{\mathrm{dd}}(r)$, and demanding that this operator in Eq. (2.19) gives the known static structure function, we obtain the relationship

$$S(q) = S_{\mathrm{F}}(q)[1 + \tilde{\Gamma}_{\mathrm{dd}}(q)S_{\mathrm{F}}(q)] \tag{4.1}$$

as a *definition* of $\tilde{\Gamma}_{\mathrm{dd}}(q)$ in terms of $S(q)$. We adopt this view here and define the "best" local approximation for $\mathcal{N}(1,2)$ such that it reproduces the best known $S(q)$. Since the exact

$S(q)$ contains a summation of exchange terms, this implies that their contribution to $S(q)$ is mimicked by a local contribution to $\tilde{\Gamma}_{\rm dd}(q)$.

An "optimal" local approximation for the effective interaction $\mathcal{W}(1,2)$ can be obtained along similar lines. From Eqs. (2.14) and (2.11) we have

$$H'_{0,pp'hh'} = W_{0,pp'hh'} + \frac{1}{2}(e_{ph} + e_{p'h'})N_{0,pp'hh'}. \quad (4.2)$$

The ground-state Euler equation for pair correlations Eq. (2.20) implies that the Fermi sea average of $H'_{0,pp'hh'}$ vanishes. Postulating a local $\mathcal{W}(1,2) \approx W(r_{12})$, consistency relates this quantity to the local approximation of $\mathcal{N}(1,2)$. This leads to[28]

$$\tilde{W}(q) = -\frac{t(q)}{S_{\rm F}(q)}\tilde{\Gamma}_{\rm dd}(q). \quad (4.3)$$

Our procedure of using the relationships in Eqs. (2.19) and (2.20) to construct local approximations for $N_{0,pp'hh'}$ and $W_{0,pp'hh'}$ can be generalized to a systematic definition of optimal local approximations for the matrix elements of any nonlocal d-body operator. Averaging the matrix elements, which depend on d particle and d hole momenta, over the Fermi sea, generates functions of the momentum transfers $\mathbf{q}_i \equiv \mathbf{p}_i - \mathbf{h}_i$ only. Spelling out Fermi occupation functions $n_{\mathbf{h}}$ and $\bar{n}_{\mathbf{p}} \equiv 1 - n_{\mathbf{p}}$ explicitly, this reads for a one-body quantity

$$O_{\mathbf{q}} \equiv \frac{\sum_h \bar{n}_{\mathbf{p}} n_{\mathbf{h}} O_{0,ph}}{\sum_h \bar{n}_{\mathbf{p}} n_{\mathbf{h}} 1} = \frac{1}{NS_{\rm F}(q)} \sum_h \bar{n}_{\mathbf{h}+\mathbf{q}} n_{\mathbf{h}} O_{0,ph}. \quad (4.4)$$

The extension to d variables is obvious,

$$O_{\mathbf{q}_1,\ldots,\mathbf{q}_d} = \sum_{h_1,\ldots,h_d} \prod_{i=1}^{d} \frac{\bar{n}_{\mathbf{p}_i} n_{\mathbf{h}_i}}{NS_{\rm F}(q_i)} O_{0,p_1,\ldots,p_d h_1,\ldots,h_d}, \quad (4.5)$$

as is the extension to matrix elements $O_{\mathbf{m},\mathbf{n}\neq\mathbf{o}}$.

We emphasize again that the quantities $O_{\mathbf{q}_1,\ldots,\mathbf{q}_d}$ contain all exchange and correlation effects in a localized manner. Therefore, effects related to the z_{ph}, as well as CBF corrections to the e_{ph}, are already part of $\tilde{W}(q)$ and $\tilde{\Gamma}_{\rm dd}(q)$. This implies, among others,

$$M_{p'h',ph} \approx \delta_{p,p'}\delta_{h,h'} + \langle hp'|\Gamma_{\rm dd}|ph'\rangle, \quad (4.6)$$

and the relationship Eq. (3.51) between the supermatrices $\mathbf{C}$ and $\mathbf{N}$ simplifies to

$$\mathbf{C} = \mathbf{1} + \frac{1}{2}\mathbf{N}. \quad (4.7)$$

B. Matrix elements

The localization procedure discussed above for $\mathcal{N}(1,2)$ implies

$$\mathbf{N} = \frac{1}{N}\tilde{\Gamma}_{\rm dd}(q)\begin{pmatrix} \delta_{\mathbf{q},+\mathbf{q}'} & \delta_{\mathbf{q},-\mathbf{q}'} \\ \delta_{\mathbf{q},-\mathbf{q}'} & \delta_{\mathbf{q},+\mathbf{q}'} \end{pmatrix} \bar{n}_{\mathbf{p}}\bar{n}_{\mathbf{p}'}n_{\mathbf{h}}n_{\mathbf{h}'}. \quad (4.8)$$

To simplify the notation, the $\delta_{\mathbf{q},\pm\mathbf{q}'}$ functions, together with the Fermi occupation numbers, are understood to be implicit in all the matrices from now on. Matrix products, i.e., sums over particle-hole labels, reduce to factors $S_{\rm F}(q)$. The inverse of $\mathbf{C}$ is readily obtained from Eq. (4.7) as

$$\mathbf{C}^{-1} = \mathbf{1} - \frac{1}{2N}\tilde{X}_{\rm dd}(q)\begin{pmatrix} 1 & 1 \\ 1 & 1 \end{pmatrix} \quad (4.9)$$

with

$$\tilde{X}_{\rm dd}(q) = \frac{\tilde{\Gamma}_{\rm dd}(q)}{1 + S_{\rm F}(q)\tilde{\Gamma}_{\rm dd}(q)}. \quad (4.10)$$

In the spirit of the discussion in Sec. IV A, this is our definition of $\tilde{X}_{\rm dd}(q)$. According to Eq. (A11), it can also be identified with the sum of all non-nodal diagrams.

Multiplying $\mathbf{C}^{-1}$ from both sides to Eq. (3.57) yields the ω-dependent effective interactions,

$$\mathbf{V}_{\text{p-h}}(\omega) = \frac{1}{N}\begin{pmatrix} \tilde{V}_{\rm A}(q;\omega) & \tilde{V}_{\rm B}(q;\omega) \\ \tilde{V}^*_{\rm B}(q;-\omega) & \tilde{V}^*_{\rm A}(q;-\omega) \end{pmatrix}. \quad (4.11)$$

To summarize, the localization of $\mathcal{N}(1,2)$ in an $S(q)$ conserving manner has *uniquely* fixed the functions $\tilde{\Gamma}_{\rm dd}(q)$ and $\tilde{X}_{\rm dd}(q)$ and, consequently, the corresponding matrices $\mathbf{N}$ and $\mathbf{C}^{-1}$. Calculating $\mathbf{V}_{\text{p-h}}(\omega)$ from Eq. (3.57) has thus been reduced to calculating $V_{\rm A,B}(q;\omega)$ from $\mathbf{W}$.

In order to derive the explicit expressions, we need the optimal local form of Eq. (3.43). This involves two steps, calculating the localized versions of the three-body vertices $K_{ph,p'p''h'h''}$ and $K^{(ph)}_{p'p''h'h'',0}$, and deriving the inverse of the four-body energy matrix $[E(\omega)]^{-1}$. We expect these quantities to be sufficiently accurate within the convolution approximation, since improving on this only marginally changes the results[7] for bosons.

The details of the derivation of the local three-body vertices $\tilde{K}_{q,q'q''}$ and $\tilde{K}^{(q)}_{q'q'',0}$ defined in Eqs. (3.34)–(3.36) can be found in Appendix B 3. These are

$$\tilde{K}_{q,q'q''} = \frac{\hbar^2}{2m}\frac{S(q')S(q'')}{S_{\rm F}(q)S_{\rm F}(q')S_{\rm F}(q'')}[\mathbf{q}\cdot\mathbf{q}'\tilde{X}_{\rm dd}(q') + \mathbf{q}\cdot\mathbf{q}''\tilde{X}_{\rm dd}(q'') - q^2\tilde{u}_3(q,q',q'')] + \left[1 - \frac{S_{\rm F}(q')S_{\rm F}(q'')}{S(q')S(q'')}\right]^{-1}\tilde{K}^{(q)}_{q'q'',0}, \quad (4.12)$$

$$\tilde{K}^{(q)}_{q'q'',0} = \frac{\hbar^2}{4m}\tilde{\Gamma}_{\rm dd}(q)\left[\frac{S(q')S(q'')}{S_{\rm F}(q')S_{\rm F}(q'')} - 1\right]\left\{\frac{q^2 S^{(3)}_{\rm F}(q,q',q'')}{S_{\rm F}(q)S_{\rm F}(q')S_{\rm F}(q'')} + \left[\frac{\mathbf{q}\cdot\mathbf{q}'}{S_{\rm F}(q')} + \frac{\mathbf{q}\cdot\mathbf{q}''}{S_{\rm F}(q'')}\right]\right\}. \quad (4.13)$$

Here, $S^{(3)}_{\rm F}(q,q',q'')$ is the three-body static structure function of noninteracting fermions, defined in Eq. (B8), and $\tilde{u}_3(q,q',q'')$ is the ground-state triplet correlation function.[28]

The implicit momentum-conservation functions $\delta_{\pm\mathbf{q},\mathbf{q}'+\mathbf{q}''}$ ensure that both vertices depend on the magnitudes of the three arguments only.

Going back to the Lagrangian, we realize that the term $\tilde{K}^{(q)}_{q'q'',0}$ is the coefficient function of the contributions to $\mathcal{L}'^{(12)}(t)$ containing $U_1(t)U_2(t)$ which we expect to be small. Our numerical applications to be discussed below will support this expectation. However, the vertex $\tilde{K}_{q,q'q''}$ contains a term of the same form. Neglecting $\tilde{K}^{(q)}_{q'q'',0}$ should, for consistency, also mean neglecting the same term in $\tilde{K}_{q,q'q''}$ which is then given by the very simple first part of Eq. (4.12). In this term we recover, apart from $S_F(q)$ factors, also the Bose version of the three-body vertex.

C. Effective interactions

Next, the matrix elements Eqs. (4.12) and (4.13) are used in Eq. (3.43) to calculate the dynamic parts of $\mathbf{W}$,

$$W_{ph,p'h'}(\omega)=\frac{\delta_{\mathbf{q},\mathbf{q}'}}{N}[\tilde{W}(q)+\tilde{W}_{\mathrm{A}}(q;\omega)],$$

$$W_{php'h',0}(\omega)=\frac{\delta_{\mathbf{q},-\mathbf{q}'}}{N}[\tilde{W}(q)+\tilde{W}_{\mathrm{B}}(q;\omega)], \tag{4.14}$$

where the energy-independent part $\tilde{W}(q)$ has been defined in Eq. (4.3). Because of the locality of the three-body matrix elements, we can write for the first dynamic contribution to Eq. (3.43),

$$\begin{aligned}&\sum_{p_1p_2h_1h_2}\sum_{p_1'p_2'h_1'h_2'}K_{ph,p_1p_2h_1h_2}[E(\omega)^{-1}]_{p_1p_2h_1h_2,p_1'p_2'h_1'h_2'}\\&\quad\times K_{p_1'p_2'h_1'h_2',p'h'}\\&=\frac{1}{N^2}\sum_{q_1q_1'}\tilde{K}_{q,q_1q_2}\tilde{K}_{q_1'q_2',q}\frac{1}{N^2}\sum_{h_1h_2h_1'h_2'}[E(\omega)^{-1}]_{p_1p_2h_1h_2,p_1'p_2'h_1'h_2'}\\&=\frac{1}{N^2}\sum_{q_1q_2}\tilde{K}_{q,q_1q_2}\tilde{E}^{-1}(q_1,q_2;\omega)\tilde{K}_{q_1q_2,q}\end{aligned} \tag{4.15}$$

with implicit factors $\delta_{\mathbf{q},\mathbf{q}_1+\mathbf{q}_2}\delta_{\mathbf{q},\mathbf{q}_1'+\mathbf{q}_2'}$ for momentum conservation. The other contributions to Eq. (3.43) are calculated analogously. The inverse four-body energy matrix and the pair propagator

$$\frac{1}{N^2}\sum_{hh'h''h'''}[E(\omega)^{-1}]_{pp'hh',p''p'''h''h'''}\equiv\delta_{q,q''}\delta_{q',q''}\tilde{E}^{-1}(q,q';\omega) \tag{4.16}$$

are calculated and discussed in Appendix C. Basically, the pair spectrum is built from two particle-hole spectra. These are, however, not centered around free particle spectra but around the Feynman dispersion relation. Consequently, our pair propagator also includes *two-phonon* intermediate states.

The resulting expressions for the energy-dependent $\tilde{W}_{\mathrm{A,B}}(q;\omega)$ are then

$$\tilde{W}_{\mathrm{A}}(q;\omega)=\frac{1}{2N}\sum_{\mathbf{q}'\mathbf{q}''}[|\tilde{K}_{q,q'q''}|^2\tilde{E}^{-1}(q',q'';\omega)+|\tilde{K}^{(q)}_{q'q'',0}|^2\tilde{E}^{-1*}(q',q'';-\omega)], \tag{4.17}$$

$$\tilde{W}_{\mathrm{B}}(q;\omega)=\frac{1}{2N}\sum_{\mathbf{q}'\mathbf{q}''}\{\tilde{K}^{(q)}_{q'q'',0}\tilde{K}_{q,q'q''}[\tilde{E}^{-1}(q',q'';\omega)+\tilde{E}^{-1*}(q',q'';-\omega)]\}. \tag{4.18}$$

Similar to the boson theory, the dynamic parts of the interactions are expressed in terms of three-body vertices and an energy denominator, the latter now being "spread" over the whole width of a two-particle-two-hole band.

The last step in our formal derivations is the calculation of $\mathbf{V}_{\text{p-h}}(\omega)$. Carrying out the operations in Eq. (3.57) yields the energy-dependent, but local functions

$$\tilde{V}_{\mathrm{A}}(q;\omega)=\tilde{V}_{\text{p-h}}(q)+[\sigma_q^+]^2\tilde{W}_{\mathrm{A}}(q;\omega)+[\sigma_q^-]^2\tilde{W}^*_{\mathrm{A}}(q;-\omega)+\sigma_q^+\sigma_q^-[\tilde{W}_{\mathrm{B}}(q;\omega)+\tilde{W}^*_{\mathrm{B}}(q;-\omega)], \tag{4.19}$$

$$\tilde{V}_{\mathrm{B}}(q;\omega)=\tilde{V}_{\text{p-h}}(q)+[\sigma_q^+]^2\tilde{W}_{\mathrm{B}}(q;\omega)+[\sigma_q^-]^2\tilde{W}^*_{\mathrm{B}}(q;-\omega)+\sigma_q^+\sigma_q^-[\tilde{W}_{\mathrm{A}}(q;\omega)+\tilde{W}^*_{\mathrm{A}}(q;-\omega)] \tag{4.20}$$

with $\sigma_q^{\pm}\equiv[S_{\mathrm{F}}(q)\pm S(q)]/2S(q)$.

V. DENSITY-DENSITY RESPONSE FUNCTION

A. General form

We now derive the density-density response function $\chi(q;\omega)$. The final result for the dynamic effective interactions, Eqs. (4.19) and (4.20), is inserted into Eq. (3.58), which is solved for $\delta\mathbf{c}$. The induced density is then obtained from Eq. (3.47). Using $\tilde{\rho}^{\mathrm{F}}_{0,ph}(\mathbf{r})=\frac{\rho}{N}e^{-i(\mathbf{p}-\mathbf{h})\mathbf{r}}$ we obtain

$$\delta\rho(q;\omega)=\frac{\rho}{2}\sum_h[z_{\mathbf{h}+\mathbf{q},\mathbf{h}}\delta c^{(1+)}_{\mathbf{h}+\mathbf{q},\mathbf{h}}(\omega)\bar{n}_{\mathbf{h}-\mathbf{q}}+z_{\mathbf{h}-\mathbf{q},\mathbf{h}}\delta c^{(1-)}_{\mathbf{h}-\mathbf{q},\mathbf{h}}(\omega)\bar{n}_{\mathbf{h}+\mathbf{q}}], \tag{5.1}$$

$$\approx\frac{NS_{\mathrm{F}}(k)\rho}{2}[\delta c^{(1+)}(q;\omega)+\delta c^{(1-)}(q;\omega)], \tag{5.2}$$

where we abbreviate in the second line $\delta c^{(1\pm)}(q;\omega)\equiv\frac{1}{N}\sum_h\delta c^{(1\pm)}_{ph}(\omega)$. Spelling out Eq. (3.58) explicitly,

$$2\tilde{h}^{\mathrm{F}}_{0,ph}(\omega)=[\pm(\hbar\omega+i\eta)-e_{ph}]\delta c^{(\pm)}_{ph}(\omega)-\tilde{V}_{\mathrm{A}}(q;\omega)\delta c^{(\pm)}(q;\omega)-\tilde{V}^*_{\mathrm{B}}(q;-\omega)\delta c^{(\mp)}(q;\omega), \tag{5.3}$$

dividing by $(\pm(\hbar\omega+i\eta)-e_{ph})$ and summing over h yields

$$\delta c^{(1\pm)}(q;\omega) = \left[\frac{2}{N}\tilde{h}_{\text{ext}}(q;\omega) + \tilde{V}_{\text{A}}(q;\omega)\delta c^{(1\pm)}(q;\omega) + \tilde{V}^{*}_{\text{B}}(q;-\omega)\delta c^{(1\mp)}(q;\omega) \right] \begin{Bmatrix} \kappa_0(q;\omega) \\ \kappa^{*}_0(q;-\omega) \end{Bmatrix} \tag{5.4}$$

with the positive-energy Lindhard function

$$\kappa_0(q;\omega) \equiv \frac{1}{N}\sum_h \frac{\bar{n}_{\mathbf{p}} n_{\mathbf{h}}}{\hbar\omega - e_{ph} + i\eta} \tag{5.5}$$

which is related to the full Lindhard function by

$$\chi_0(q;\omega) = \kappa_0(q;\omega) + \kappa^{*}_0(q;-\omega). \tag{5.6}$$

Solving for $\delta c^{(1\pm)}(q;\omega)$ and inserting into Eq. (5.1) we obtain for $\chi(q;\omega)$

$$\chi(q;\omega) = N(q;\omega)/D(q;\omega),$$

$$N(q;\omega) = \kappa_0(q;\omega) + \kappa^{*}_0(q;-\omega) - \kappa_0(q;\omega)\kappa^{*}_0(q;-\omega)[\tilde{V}_{\text{A}}(q;\omega) + \tilde{V}^{*}_{\text{A}}(q;-\omega) - \tilde{V}_{\text{B}}(q;\omega) - \tilde{V}^{*}_{\text{B}}(q;-\omega)],$$

$$D(q;\omega) = 1 - \kappa_0(q;\omega)\tilde{V}_{\text{A}}(q;\omega) - \kappa^{*}_0(q;-\omega)\tilde{V}^{*}_{\text{A}}(q;-\omega) + \kappa_0(q;\omega)\kappa^{*}_0(q;-\omega)[\tilde{V}_{\text{A}}(q;\omega)\tilde{V}^{*}_{\text{A}}(q;-\omega) - \tilde{V}_{\text{B}}(q;\omega)\tilde{V}^{*}_{\text{B}}(q;-\omega)]. \tag{5.7}$$

Equation (5.7) is the TDHF response function for local- and energy-dependent interactions. Evidently, the conventional RPA form Eq. (1.7) can only be recovered if the interactions $\tilde{V}_{\text{A}}(q;\omega)$ and $\tilde{V}_{\text{B}}(q;\omega)$ are *energy independent* and *equal*. Clearly, our result in Eq. (5.7) significantly differs from Eq. (1.7) with $\tilde{V}_{\text{p-h}}(q)$ simply replaced by some energy-dependent $\tilde{V}_{\text{p-h}}(q;\omega)$. Such an RPA-like form for the density-density response function lacks microscopic justification.

B. Long-wavelength limit

In the limit $q \to 0$, the spectrum is dominated by collective excitations, e.g., zero sound or plasmons. Both vertices in Eqs. (4.12) and (4.13) vanish linearly in q, hence $\tilde{W}_{\text{A}}(q;\omega)$ and $\tilde{W}_{\text{B}}(q;\omega)$ are quadratic in q as $q \to 0$.

For neutral systems, the dynamic corrections to the effective interactions $\tilde{V}_{\text{A,B}}(q;\omega)$ in Eqs. (4.19) and (4.20) are therefore negligible in the long-wavelength limit. The long-wavelengths density-density response function is then given by its RPA form Eq. (1.7) with the static particle-hole interaction $\tilde{V}_{\text{p-h}}(q)$. The zero-sound speed c_0 is determined by the long-wavelength solution of the RPA equation.

For charged quantum fluids, $\sigma^{\pm}_q \approx S_{\text{F}}(q)/2S(q)$, hence $\tilde{V}_{\text{A}}(q,\omega) = \tilde{V}_{\text{B}}(q,\omega)$, which again implies the RPA form Eq. (1.7)

$$\chi(q;\omega) = \frac{\chi_0(q;\omega)}{1 - \chi_0(q;\omega)\tilde{V}_{\text{A}}(q;\omega)} \quad \text{as} \quad q \to 0. \tag{5.8}$$

However, now the effective interaction is

$$\tilde{V}_{\text{A}}(q;\omega) = \tilde{V}_{\text{p-h}}(q) + \frac{S^2_{\text{F}}(q)}{4S^2(q)}[\tilde{W}_{\text{A}}(q;\omega) + \tilde{W}_{\text{A}}(q;-\omega) + \tilde{W}_{\text{B}}(q;\omega) + \tilde{W}_{\text{B}}(q;-\omega)] \quad \text{as} \quad q \to 0. \tag{5.9}$$

The static particle-hole interaction approaches the Coulomb potential $\tilde{v}_{\text{c}}(q) = 4\pi e^2/q^2$

$$\tilde{V}_{\text{p-h}}(q) = \tilde{v}_{\text{c}}(q) + V_0 \quad \text{as} \quad q \to 0. \tag{5.10}$$

We can therefore write Eq. (5.9) as

$$\tilde{V}_{\text{A}}(q;\omega) = \tilde{V}_{\text{B}}(q;\omega) = \tilde{v}_{\text{c}}(q) + V_0(\omega) \quad \text{as} \quad q \to 0. \tag{5.11}$$

As for charged bosons,[36] the two-pair fluctuations modify the RPA result. The static potential $\tilde{V}_{\text{p-h}}(q)$ and $\tilde{W}_{\text{A,B}}(q;\omega)$ contribute for $q \to 0$ at the same level.

C. Static response function

$\tilde{E}^{-1}(q,q';\omega=0)$ is real and negative, this is most easily seen from the representation Eq. (C9). Therefore, all interactions $\tilde{W}_{\text{A,B}}(q;0)$ in Eqs. (4.17) and (4.18) and $\tilde{V}_{\text{A,B}}(q;0)$ in Eqs. (4.19) and (4.20) are real. The response function Eq. (5.7) can again be cast into the RPA form

$$\chi(q;0) = \frac{\chi_0(q;0)}{1 - \tilde{V}_{\text{stat}}(q)\chi_0(q;0)} \tag{5.12}$$

with a static effective interaction

$$\tilde{V}_{\text{stat}}(q) \equiv \tilde{V}_{\text{p-h}}(q) + \frac{S^2_{\text{F}}(q)}{2S^2(q)}[\tilde{W}_{\text{A}}(q;0) + \tilde{W}_{\text{B}}(q;0)]. \tag{5.13}$$

Unlike Eq. (5.9), this form holds for all wavelengths.

For *short wavelengths* the static response function has the asymptotic form[37,38]

$$\chi(q \to \infty;0) = -\frac{2}{t(q)} - \frac{8}{3t^2(q)}\frac{\langle \hat{T} \rangle}{N} + \mathcal{O}(q^{-5}), \tag{5.14}$$

where $\langle \hat{T} \rangle$ is the kinetic energy. In the RPA, one obtains in Eq. (5.14) only the kinetic energy of the noninteracting system. To obtain the correct asymptotic form, it is therefore necessary to include pair and, possibly, higher order fluctuations.

Again, we know the result for bosons as a guide: treating pair fluctuations in the "convolution" approximation leads to the correct asymptotic behavior with $\langle \hat{T} \rangle$ in Eq. (5.14) given in that approximation.[18]

We show in Appendix D that

$$\tilde{V}_{\rm stat}(q\to\infty)=\frac{1}{2}\tilde{W}_{\rm A}(q\to\infty;0)=-\frac{2}{3}\frac{\langle T\rangle^{\rm CA}-T_{\rm F}}{N}, \tag{5.15}$$

where $\langle T\rangle^{\rm CA}$ is the kinetic energy in "uniform limit" or convolution approximation Eq. (A10). Hence, inserting the short-wavelength expansion of the Lindhard function, the static response function Eq. (5.12) indeed assumes the form Eq. (5.14)

$$\chi(q;0)=-\frac{2}{t(q)}-\frac{8}{3t^2(q)}\frac{\langle T\rangle^{\rm CA}}{N}\quad \text{as}\quad q\to\infty \tag{5.16}$$

with the kinetic energy being calculated in the uniform limit approximation Eq. (A10).

VI. APPLICATIONS

A. Dynamic structure of ^{3}He

1. Motivation

The helium fluids are the prime examples of strongly correlated quantum many-body systems. They have been studied for decades and still offer surprises leading to new insight. It is fair to say that understanding the helium fluids lies at the core of understanding other strongly correlated systems. The most important and most interesting field of application of our theory is therefore liquid ^{3}He.

Recent developments[7,39] have brought manifestly microscopic theories of ^{4}He to a level where quantitative predictions of the excitation spectrum are possible far beyond the roton minimum without any information other than the underlying microscopic Hamiltonian (2.1). ^{3}He is the more challenging substance for both, theoretical and experimental investigations. Experimentally, the dynamic structure function $S(q;\omega)$ of ^{3}He is mostly determined by neutron scattering. The results are well documented in a book,[40] the theoretical and experimental understanding a decade ago has been summarized in Ref. 25. Recent inelastic x-ray scattering experiments have led to a controversy on the evolution of the zero sound mode at intermediate wave vectors,[41–43] we will comment on this issue below.

The RPA Eq. (1.7) suggests that $S(q;\omega)$ can be characterized as a superposition of a collective mode similar to the phonon maxon roton in ^{4}He, *plus* an incoherent particle-hole band which strongly dampens this mode.[44] The picture is *qualitatively* adequate but misses some important *quantitative* physics. In ^{3}He the RPA, when defined through the form Eq. (1.7) and such that the sum rules in Eqs. (1.4) and (1.5) are satisfied, predicts a zero-sound mode that is significantly too high. This is consistent with the same deficiency of the Feynman spectrum Eq. (1.6) in ^{4}He. Drawing on the analogy to ^{4}He,[44] the cure for the problem is, as pointed out above, to include pair fluctuations $\delta u^{(2)}_{pp'hh'}(t)$ in the excitation operator.

An alternative, namely, to lower the collective mode's energy by introduction of an effective mass in the Lindhard function, leads to various difficulties. First, one violates the sum rules in Eqs. (1.4) and (1.5), i.e., one disregards well-established information on the system. Second, the effective mass is far from constant; it has a strong peak around the Fermi momentum,[45–48] a secondary maximum around $2k_{\rm F}$, and then quickly falls off to the value of the bare mass. In fact, it is not even clear if the notion of a "single (quasi)particle spectrum" that is characterized by a momentum is adequate at these wave numbers.

The localization procedure of Sec. IV implies that the only input needed for the application of our theory is the static structure function $S(q)$ whereas the single-particle spectrum is that of a free particle. We hasten to state that we do *not* claim that the precise location of the single-particle spectrum is completely irrelevant for the energetics of the zero sound; we only claim that the *dominant mechanism* in Bose and Fermi fluids is the same, namely, pair fluctuations. In order to maintain the sum rules in Eqs. (1.4) and (1.5), any modification of the particle-hole spectrum must go along with an inclusion of exchange effects. At the level of single-particle fluctuations,[4,5] such a calculation is quite feasible.[49,50] However, to describe the dynamics of ^{3}He correctly, it is insufficient to include only the CBF single-particle energies Eq. (2.14). These suggest a smooth spectrum with an effective mass slightly less than the bare mass, in contradiction to the highly structured spectrum mentioned already above.

2. Collective mode

For our calculations we have used input from the FHNC-EL calculations of Ref. 28 that utilizes the Aziz-II potential[51] and includes optimized triplet correlations as well as four- and five-body elementary diagrams. An overview of our results for bulk ^{3}He and a comparison with both the RPA and experimental data is shown in Fig. 1 for four different densities. The most prominent consequence of pair fluctuations is a change in energy and strength of the collective mode and its continuation into the particle-hole band. Pair fluctuations also contribute a continuum background outside the particle-hole continuum.

At long wavelengths, the collective mode is sharp and well defined above the particle-hole band, exhausting most of the sum rules in Eqs. (1.4) and (1.5). In this regime, the RPA provides a faithful description of the physics. This is in accordance with the observation that the dynamic correction to the effective interactions vanish, for neutral systems, in the long-wavelength limit. With increasing density, the speed of sound increases and the phonon becomes farther separated from the particle-hole band.

Further details are shown in Fig. 2. At intermediate wavelengths the collective mode bends down due to the attractiveness of the effective interaction. This is where the dynamic theory starts to deviate visibly from the RPA. Evidently, pair fluctuations are the major cause for lowering the energy of the collective mode, although they do not completely bridge the discrepancy between the RPA and experiments.[24,25] This is expected because, for bosons, pair fluctuations bridge only about two thirds of the gap between the Feynman and the experimental roton energy.[7,17] Three-body and higher-order fluctuations are also important.[18] We expect that these cor-

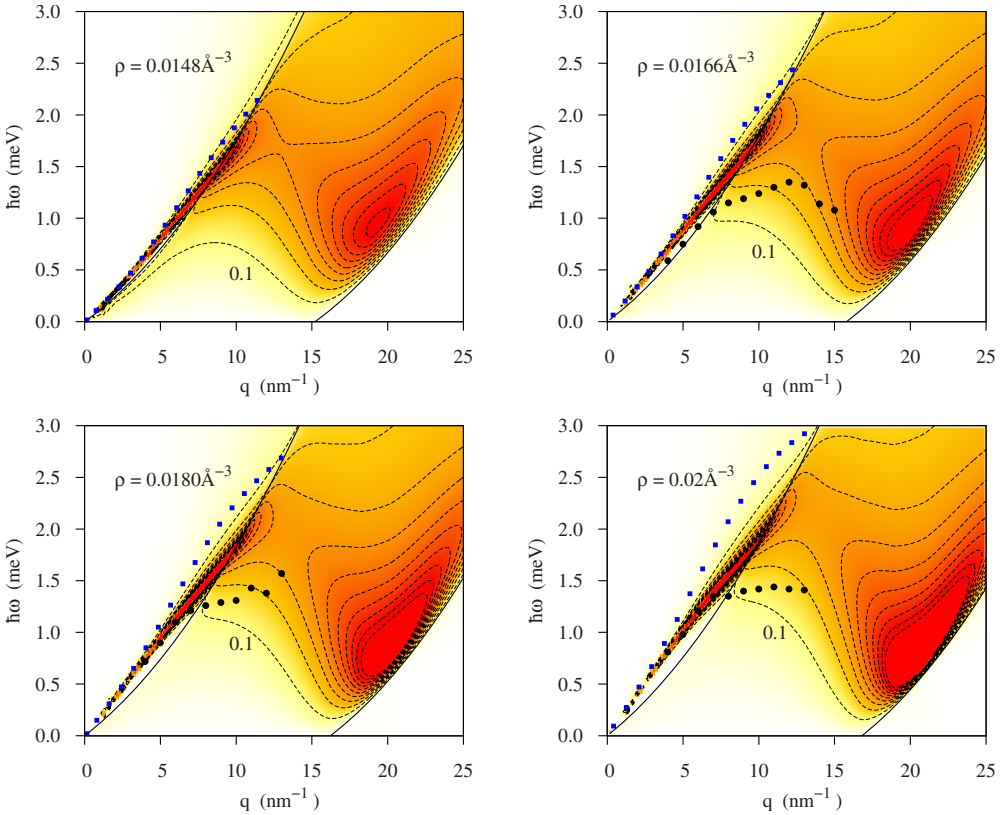

FIG. 1. (Color online) $-\Im m\chi(q;\omega)$ of ^{3}He, for the densities ρ=0.0148, 0.0166, 0.018, and 0.02 Å^{-3}. The experimental results for the collective mode (dots) are from inelastic neutron-scattering experiments at the ILL (Ref. 24). The densities 0.0166, 0.0180, and 0.0200 Å^{-3} correspond in good approximation to the pressures p=0, 5, and 10 bar (Refs. 52 and 53). Dashed lines are equidistant contours at $0.1, 0.2, \ldots, 1.0 t_F^{-1}$ marking the same absolute value in all plots. Solid lines are the boundaries of the particle-hole continuum for $m^*=m$. The blue boxes show the RPA result for the collective mode.

rections are smaller in ^{3}He due to its lower density, yet not negligible.

When the collective mode enters the particle-hole band, a slight kink in the position of the maximum in $S(q;\omega)$ is expected, as well as an abrupt broadening of the mode. At saturated vacuum pressure, shown in the left part of Fig. 2, these effects are difficult to identify in the experiments.[25] A possible reason is that the observed mode stays always very close to the particle-hole band. The measured mode width in Fig. 2 gives no clear indication of the upper boundary of the particle-hole band other than that it is determined by a spectrum with an average effective mass of $m^* \lessapprox m$.

The situation is much clearer at higher pressure. With increasing density, the speed of sound increases, separating the collective mode farther from the particle-hole band. For ρ=0.02 Å^{-3} a clear kink is identified at $q \approx 5$ nm^{-1} (Fig. 2 right part). The broadening is also more abrupt and, in particular, does not increase for larger values of q. Similar to saturated vapor pressure, explaining these data requires a boundary of the particle-hole band that is even above that of the noninteracting Fermi fluid. Damping due to multiparticle excitations is, on the other hand, for both densities far too small to account for the experimentally seen broadening of the zero sound mode.

3. Frequency dependence of $S(q;\omega)$

For a quantitative discussion we show in Fig. 3 the dynamic structure factor as a function of frequency at a se-

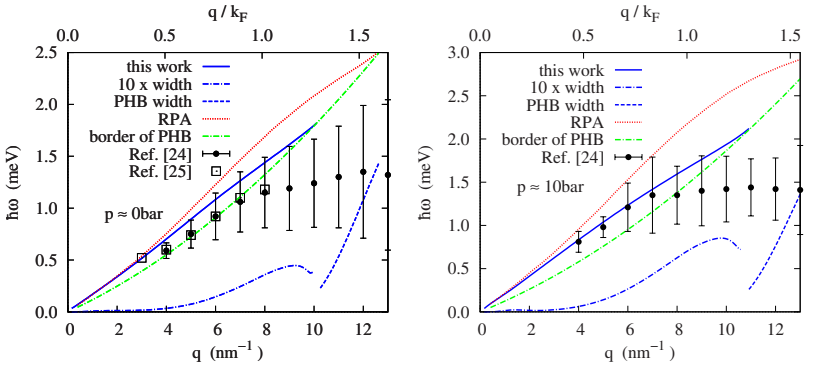

FIG. 2. (Color online) Zero-sound mode calculated within the pair-fluctuation theory (full blue line), RPA [dashed red line], and experimental data by the ILL group, Ref. 25 (square symbols) and Ref. 24 (circles). The bars indicate the width of the fit to the data, the line at the bottom of the figure gives the width due to pair fluctuations enhanced by a factor of 10 to make it visible. The dashed blue line gives the full width at half maximum of the mode within the particle-hole continuum. Left part: ρ=0.0166 Å^{-3}, right part: ρ=0.02 Å^{-3}.

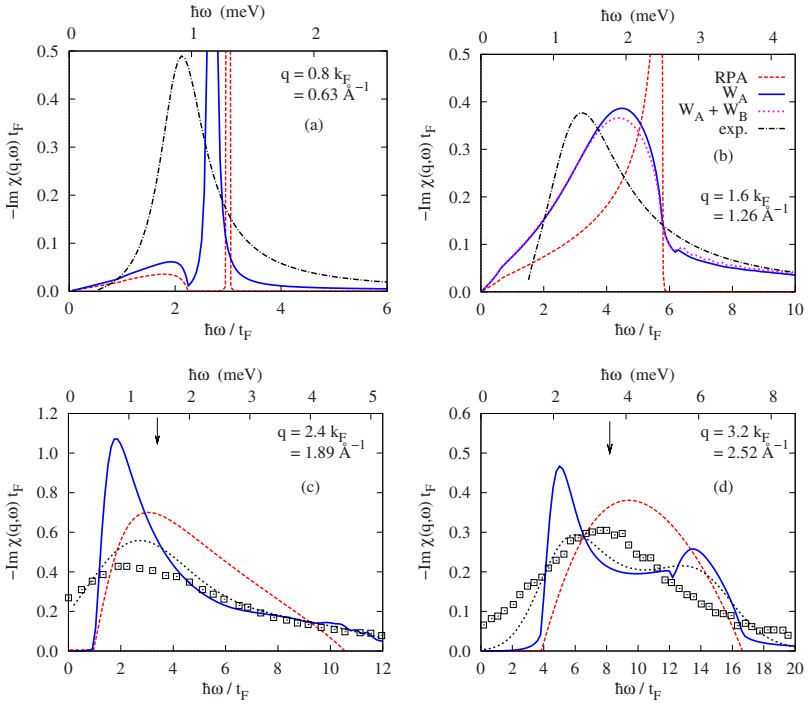

FIG. 3. (Color online) [(a)–(d)] $-\Im m\chi(q;\omega)$ for ^{3}He as a function of energy at $\rho=0.0166$ Å^{-3} for a sequence of momentum transfers $q=0.8$, 1.6, 2.4, $3.2k_F$. Also shown is the RPA dashed (red). The full (blue) line is the result of this work with the simplified $\tilde{W}_A(q;\omega)$ and $\tilde{W}_B(q,\omega)=0$ as discussed in the text. In panel (b), we also show the results when the full $\tilde{W}_A(q;\omega)$ and $\tilde{W}_B(q;\omega)$ of Eqs. (4.17) and (4.18) are retained (short dashed magenta line). The results from the different approximations are almost indistinguishable in panels (a)–(d) and therefore not shown. The black dashed-dotted line in panels (a) and (b) are fits to the experimental results of Ref. 24. In panels (c) and (d) we indicate the maximum of the experimentally observed dynamic structure function by an arrow. We also plot in panels (c) and (d) recent inelastic x-ray diffraction data obtained by Albergamo *et al.* (Ref. 41) (boxes) as well as our theoretical results folded with the experimental resolution (dashed line).

quence of wave vectors. We conclude that the RPA quantitatively and even qualitatively differs from our theory and the experiment. Including pair fluctuations improves the agreement with experiment significantly. The arrows in panels (c) and (d) indicate the maximum of the experimentally observed dynamic structure function.

In Fig. 3(b) we also show the consequence of the plausible simplification of our theory discussed already in connection with Eqs. (4.12) and (4.13). We neglect all terms that vanish for bosons as well as for large momentum transfers $q,q',q''\geq 2k_F$. This is $\tilde{K}^{(q)}_{q'q'',0}$ and, consequently, the second term in $K_{q,q'q''}$, Eq. (4.12). The three-body vertex is then given by the first term in Eq. (4.12), see also Eq. (D1). This simplifies the effective interactions significantly: Only the first term of Eq. (4.17) for $\tilde{W}_A(q;\omega)$ contributes and $\tilde{W}_B(q;\omega)$ is neglected. Figure 3(b) shows that these simplifications modify our results only marginally, the form Eq. (D1) can therefore be considered a practical and useful simplification of our theory.

Figures 3(c) and 3(d) show our results for the two momentum transfers $q=2.4k_F=1.89$ Å^{-1} and $q=3.2k_F=2.52$ Å^{-1}. Recent x-ray scattering experiments in that momentum range[41–43] appeared to support the notion of a high-momentum collective mode without visible damping by incoherent particle-hole excitations. Figures 3(c) and 3(d) show that pair fluctuations lead to a narrowing of the strength of $S(q;\omega)$ compared to the RPA. To facilitate the comparison with experiments, we have convoluted our result with the instrumental resolution of 1.58 meV, the results are also shown in Figs. 3(c) and 3(d). After this, our results agree quite well with the experimental spectrum. Also, the location of the observed peak intensity for $q=2.4k_F$ appears to be consistent with our calculation. The RPA is, on the other hand, too broad to explain the data. We also point out that a value of the effective mass close to $m^*\approx m$ is consistent with our theoretical calculations.[48] We have to conclude therefore that the observed width of the x-ray data are also consistent with our picture.

After a regime of strong damping we see in Fig. 1 an intensity peak at momentum transfer of $q\approx 2.5k_F$. With increasing density, this peak moves toward the lower edge of the particle-hole band and becomes sharper. Such a peak should be identified with the remnant of the roton excitation in ^{4}He, broadened by the particle-hole continuum. The overall agreement with the experiment is quite good, see Fig. 1 of Ref. 24. Our theory predicts a "roton minimum" that is slightly above the observed energy; this is expected because for bosons a similar effect is observed. To obtain a higher accuracy, triplet- and higher order fluctuations must be included.[18]

4. Static response

For completeness, and because the quantity should be obtainable by experiments and simulations similar to those for ^{4}He (Refs. 54 and 55) and on bulk jellium,[56] we show in Fig. 4 the static response function $\chi(q,0)$ of ^{3}He at $\rho=0.0166$ Å^{-3}. The main peak, which is a result of the local symmetry in the fluid, is visibly raised compared to the RPA result. We suspect, form experience with the boson theory, that this peak is still a bit underestimated.

The comparison also lets us assess the validity of an energy-independent particle-hole interaction. Figure 5 shows a comparison between the FHNC $\tilde{V}_{p\text{-}h}(q)$ and the static effective interaction Eq. (5.13). Evidently, the qualitative structure is very similar, in particular, $\tilde{V}_{p\text{-}h}(q\to 0)=\tilde{V}_{stat}(q\to 0)$ as discussed in Sec. V B. The most visible difference is that $\tilde{V}_{stat}(q)$ approaches a constant for large q, see Eqs. (5.14) and (5.15).

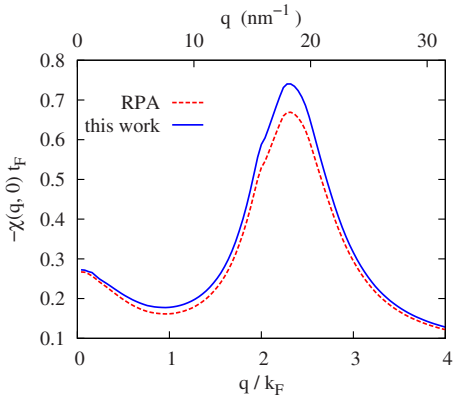

FIG. 4. (Color online) Static response of ^{3}He at $\rho = 0.0166$ Å^{-3}. The dashed (red) curve shows the RPA result whereas the full (blue) line is the result of this work.

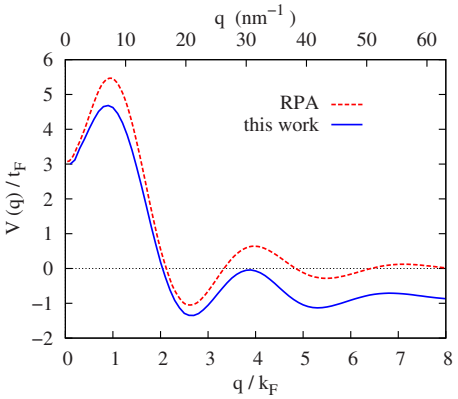

FIG. 5. (Color online) Effective interaction of ^{3}He at $\rho = 0.0166$ Å^{-3}. The dashed (red) curve shows the static effective interaction $\tilde{V}_{\text{p-h}}(q)$ whereas the full (blue) line is $\tilde{V}_{\text{stat}}(q)$.

B. Electron liquid

The second typical area of application of microscopic many-body methods is the electron liquid.[38,57] It provides the basic understanding of valence-electron correlations in simple metals. In its two-component version it has proved useful for describing the electron-hole liquid in semiconductors.

Compared to the helium fluids, the soft repulsion of the Coulomb interaction induces substantially weaker correlations. Therefore, electrons are much less challenging than ^{3}He and the RPA (or slightly modified versions) contain much of the relevant physics.

Correlations are somewhat more pronounced in layered realizations of the electron liquid, such as Si- and GaAs-AlGaAs heterostructures. For electrons on He surfaces preliminary results show[58] that at very low densities, again, a rotonlike structure evolves for intermediate wave vectors.

We have seen that pair fluctuations contribute, already at long wavelengths, to the static response function, see our discussion in Secs. V B and V C. Most important are, of course, those effects that are *qualitatively* new consequences of multiparticle fluctuations. These are the short-wavelength behavior of the static response function and the appearance of a new feature in the dynamics structure function, namely, the "double-plasmon" excitation. The latter has raised new interest[26,27] in studying the dynamics of electrons at metallic densities in this $(q;\omega)$ region.

1. Double plasmon

Figure 6 shows the dynamic structure factor $S(q;\omega)$ obtained from the pair-fluctuation theory. We have chosen two different densities $\rho \equiv 3/(4\pi r_s^3 a_B^3)$, corresponding to Al, $r_s = 2.06$ and Na, $r_s = 3.99$. Immediately obvious are the finite width (i.e., lifetime) of the plasmon above the particle-hole band and a second peaklike structure around twice the plasma frequency ω_p.

Characteristic cuts at constant wave vectors q are shown in Fig. 7 for Na. In parts (a) and (b) the plasmon is outside the particle-hole band and rather sharp; the second peak slightly above $2\hbar\omega_p = 4.5 t_F$ is clearly visible. We identify this

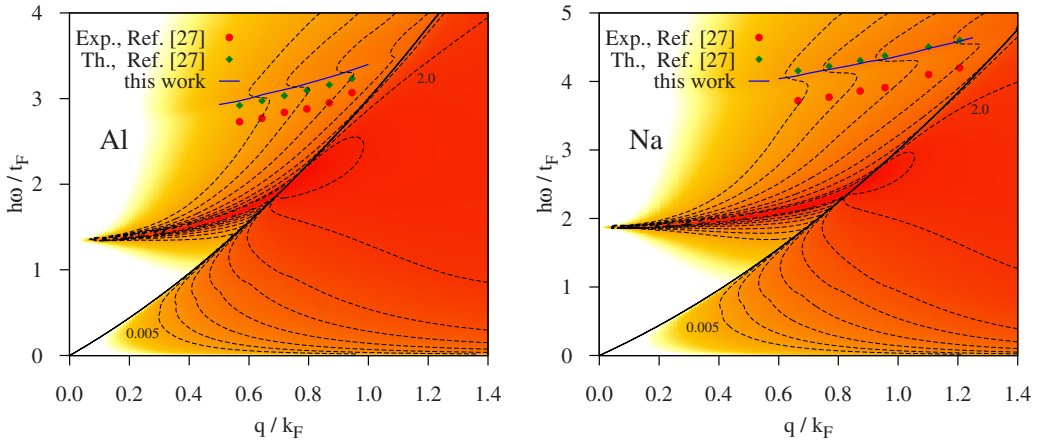

FIG. 6. (Color online) The figure shows $-\Im m\chi(q;\omega)$ of an electron liquid with density parameters $r_s = 2.06$ and $r_s = 3.99$ appropriate for Al and Na, respectively. As in Fig. 1, dark red regions correspond to high intensity (logarithmic scale). The blue line is the position of the double-plasmon peak obtained in the present work, red dots are experimental results (Ref. 27) from inelastic x-ray scattering and green diamonds results from Green's functions calculations (Refs. 27 and 59). The dashed lines are contours marking the values 0.005, 0.01, 0.02, 0.04, 0.08, 0.16, 0.5, 1.0, and 2.0 in both plots.

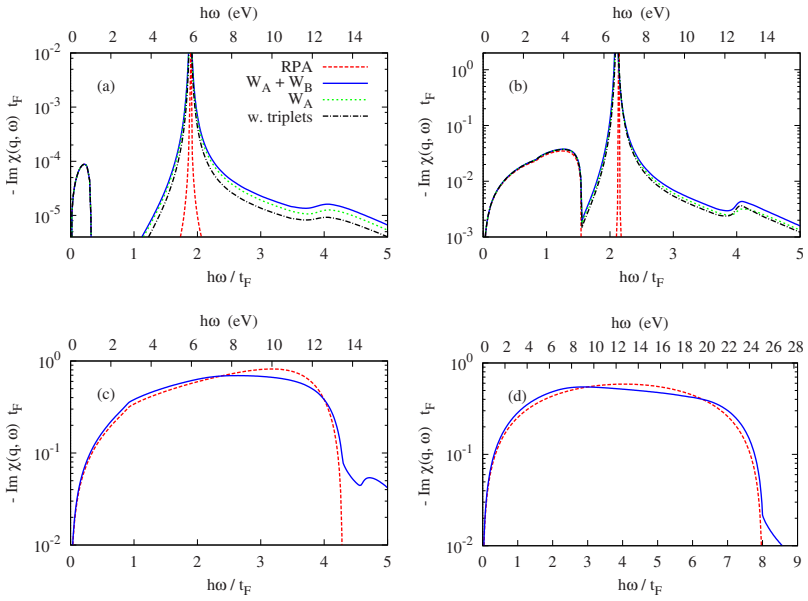

FIG. 7. (Color online) $-\Im m\chi(q;\omega)$ for Na (r_s=3.99), at wave vectors q_0 (a) $0.15k_F$, (b) $0.6k_F$, (c) $1.3k_F$, and (d) $2.0k_F$. The full (blue) lines are our pair-fluctuation theory, dashed (red) lines are the RPA results using $\tilde{V}_{p\text{-}h}(q)$. To make the plasmon visible, the RPA data have been broadened artificially by adding an imaginary frequency of 10^{-5} eV/$\hbar$. The dotted (green) lines in (a) and (b) refer to neglecting $K^{(q)}_{q'q'',0}$ in Eqs. (4.12) and (4.13) and the dashed-dotted (black) lines include ground-state triplet correlations. At larger momentum transfers these effects are too small to be visible.

feature, which has also been observed experimentally,[27] with the double-plasmon.

The double-plasmon excitation is due to the emergence of an imaginary part in $\tilde{V}_A(q\to 0,\omega)$ at $\omega\approx 2\omega_p$, caused by the appearance of an imaginary part of the pair propagator $\tilde{E}^{-1}(q',q'';\omega)$. It is therefore a genuine multipair effect. The properties of the pair propagator are discussed in Appendix C 2. From Eq. (B19) we obtain for the double-pole part of the dynamic interaction Eq. (5.9)

$$\Im m\tilde{V}_A(q\to 0;\omega)=\frac{9\hbar^2\omega_p^2}{16t_F^2}\frac{\pi}{8N}\sum_{\mathbf{q}'}\left[\frac{k_F}{q}K_{q,q'q''}\right]^2 z^2(q')\times\{\delta(2\hbar\omega_c(q')-\hbar\omega)+\delta(2\hbar\omega_c(q')+\hbar\omega)\}. \quad (6.1)$$

In Fig. 7(c), the plasmon is broad and Landau damped while the double plasmon still shows a clear structure, even at the brink of entering the particle-hole continuum. Some structure in the spectrum persists to even higher momentum transfers: At $q=2.0k_F$ in Fig. 7(d), traces of the ordinary as well as the double plasmon show up as a faint double-peak structure with its minimum where the RPA yields a single maximum.

We now investigate the nature of the slight but measurable[27] peak in the loss function at approximately twice the plasmon frequency ω_p. Figure 8 shows $S(q,\omega)$ for r_s=3.99 for three different momentum transfers, the position of the double plasmon is marked with arrows.

We have already shown in Fig. 6 the location of the double-plasmon excitation and a comparison with the experimental inelastic x-ray scattering data.[26,27] The double plasmon is also accessible by Green's function methods.[59] These results are very close to those of our pair-fluctuation theory. This can be understood from the fact that the leading terms of the long-wavelength part of the pair propagator actually contain no correlation effects, see Eq. (C30). Hence, theories that are less well suited than CBF for the description of strong correlations should, similar to the single plasmon, give the right answer. The remaining discrepancy with experiments must therefore be attributed to lattice effects. Figure 8 shows more details of $S(q,\omega)$ at a sequence of three different momentum transfers for r_s=3.99 (the position of the double plasmon is marked with arrows), in particular, in order to assess the relative strength of the double-plasmon excitation compared to the underlying continuum.

2. Static response

Monte Carlo studies of the static response function $\chi(q;0)$ were performed for two- and three-dimensional ^{4}He (Refs. 54 and 55) and on bulk jellium[56] for r_s=2, 5, and 10. While $\chi(q;\omega)$ is accessible experimentally, for electron liquids it is popular to define a *static local field correction* to the Coulomb interaction $\tilde{v}_c(q)$ via[38]

$$\tilde{V}_{stat}(q)\equiv\tilde{v}_c(q)[1-G(q)]. \quad (6.2)$$

From our analysis it is clear that a response function in the RPA form can be defined only for $q\to 0$ and at ω=0. There-

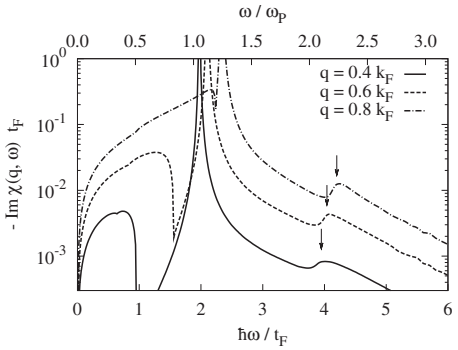

FIG. 8. Cuts of the imaginary part of the density-density response function at Na density (r_s=3.99), for constant momentum transfer $q=0.4k_F$ (solid line), $q=0.6k_F$ (dashed line), and $q=0.4k_F$ (dashed-dotted line). The arrows mark the position of the double plasmon. ω_p is the plasma frequency.

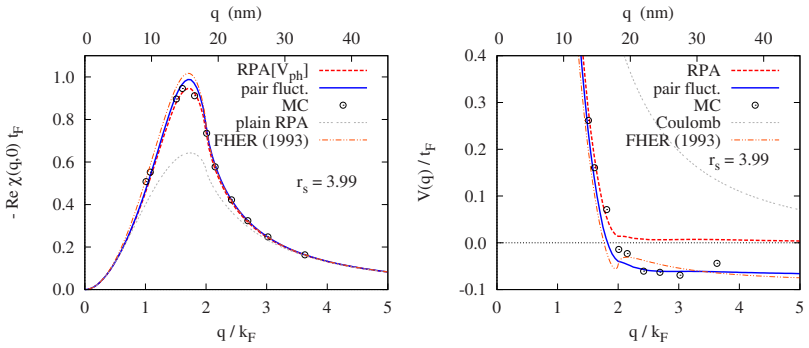

FIG. 9. (Color online) Static response function (left) and static effective interaction (right) of the electron liquid at $r_s=3.99$. Full blue lines are our results, black dashed-dotted lines a fit based on the simulations (Refs. 56 and 60). Dotted red and thin broken lines show the RPA with $\tilde{V}_{\text{p-h}}(q)$ and $\tilde{v}_{\text{c}}(q)$, respectively.

fore, only in these two cases such a function is a physically meaningful quantity.

In the $q\to\infty$ limit, our theory yields a finite value for $V_{\text{stat}}(q)$, resulting in $G(q)\propto q^2$, whereas $\tilde{V}_{\text{p-h}}(q)$ falls off like the bare potential. This correct q dependence arises *solely* from multiparticle fluctuations. In Fig. 9 we compare our results with the Monte Carlo data and with curves calculated from an analytic fit for $-v_{\text{c}}(q)G(q)$ obtained from the latter.[60] The agreement is remarkably good.

No trace of a possible "hump" in $G(q)$ around $2k_{\text{F}}$ as a remnant of some charge- or spin-density wave instability was found in the simulations, but it also was not fully conclusively ruled out. Our results, clearly, do not yield any such peak structure at $2k_{\text{F}}$ either.

VII. SUMMARY

We have presented the fermion version of theories of the dynamic response of Bose fluids that have been developed in the past successfully by Jackson, Feenberg, and Campbell. These methods form the basis of our present understanding of the dynamics of Bose fluids. Our derivations were admittedly lengthy but eventually led to a reasonably compact formulation of the dynamic response of correlated Fermi fluids. Our final result could be formulated as a set of TDHF equations in terms of dynamic and nonlocal effective interactions.

For the first applications we have reduced the theory to a practical level capturing the relevant physics while avoiding many of the technical complications. In particular the version of the equations of motion spelled out in Appendix F has proved to be adequate for systems as different as ^{3}He and homogeneous electrons. It is hardly more complicated than TDHF. The sole required input is the static structure function $S(q)$ which can, in principle, also be obtained from simulations. Our developments have led to *quantitative* improvements of our understanding of ^{3}He and electrons as well as to the description of *qualitatively new* effects such as mode-mode coupling, multiparticle spectra, and damping.

We have, at various places, commented on the role of the particle-hole spectrum. In the homogeneous electron liquid, the interaction corrections to the single-particle spectrum are relatively small,[35,61] the theory formulated here should therefore suffice for many purposes. The situation is more difficult in ^{3}He. As is seen from our results, good agreement with experiments can be reached by assuming a spectrum of non-interacting fermions. In particular looking at the zero-sound damping suggests that, at $q\approx k_{\text{F}}$, the boundary of the single-particle continuum should be close (perhaps even above) to the one given by a noninteracting spectrum, cf. Fig. 2. This is not in contradiction to experiments[52,62] suggesting an effective-mass ratio $m^*/m\approx 3$ at the Fermi surface. One reason is that the effective-mass ratio drops rapidly with distance from the Fermi surface. The more fundamental reason, however, is that the concept of describing the particle-hole excitations by a spectrum that depends on momentum only is questionable at elevated wave numbers. More precisely, the single-particle motion is described by a nonlocal, energy-dependent self-energy. Upon closer examination it becomes clear that exchange effects are intimately related to self-energy corrections and exchange effects must therefore be included simultaneously.

In independent work, we have used the ideas of CBF theory as well as the Aldrich-Pines pseudopotential theory to calculate the single-particle propagator in ^{3}He. In both three and two dimensions, we found good agreement between the theoretical effective mass near the Fermi surface and that obtained experimentally from specific-heat measurements.[47,48,63] However, the somewhat *ad hoc* use of the effective interactions in that work is still awaiting rigorous justification. This is the subject of future work.

ACKNOWLEDGMENTS

A part of this work was done while one of us (E.K.) visited the Physics Department at the University at Buffalo, SUNY. Discussions with C. E. Campbell, H. Godfrin, and R. E. Zillich are gratefully acknowledged. This work was supported, in part, by the Austrian Science Fund FWF under Project No. P21264.

APPENDIX A: GROUND-STATE THEORY

1. Essence of FHNC-EL

For the sake of the discussions of this work we here briefly review the essence of variational FHNC theory. The diagram expansion and summation procedure that is used to derive, for the variational wave function Eq. (2.2) a set of equation for the calculation and optimization of physical observables has been described at length in review articles[21] and pedagogical literature.[22] Details on the specific implementation for ^{3}He are given in Ref. 28.

Here, we spell out a reduced set of equations. These do not provide the quantitatively best implementation[28] of the FHNC-EL theory, but they contain the relevant physics: They provide, in the language of perturbation theory, a self-consistent approximate summation of ring and ladder diagrams,[29] thereby capturing both, long-ranged as well as short-ranged features.

In the simplest approximation,[64] which contains, as we shall see momentarily, the RPA expression (1.7), the Euler Eq. (2.5) can be written in the form[28]

$$S(q) = \frac{S_{\mathrm{F}}(q)}{\sqrt{1 + 2\frac{S_{\mathrm{F}}^2(q)}{t(q)}\tilde{V}_{\text{p-h}}(q)}}, \tag{A1}$$

where $t(q)=\hbar^2q^2/2m$ is the kinetic energy of a free particle and

$$V_{\text{p-h}}(r) = [1+\Gamma_{\mathrm{dd}}(r)]v(r) + \frac{\hbar^2}{m}|\nabla\sqrt{1+\Gamma_{\mathrm{dd}}(r)}|^2 + \Gamma_{\mathrm{dd}}(r)w_{\mathrm{I}}(r) \tag{A2}$$

is what we call the particle-hole interaction. Auxiliary quantities are the "induced interaction"

$$\tilde{w}_{\mathrm{I}}(q) = -t(q)\left[\frac{1}{S_{\mathrm{F}}(q)} - \frac{1}{S(q)}\right]^2\left[\frac{S(q)}{S_{\mathrm{F}}(q)} + \frac{1}{2}\right], \tag{A3}$$

and the "direct-direct correlation function"

$$\tilde{\Gamma}_{\mathrm{dd}}(q) = [S(k) - S_{\mathrm{F}}(q)]/S_{\mathrm{F}}^2(q) \tag{A4}$$

[see also Eq. (4.1)]. Equations (A1)–(A4) form a closed set which can be solved by iteration. Note that the Jastrow correlation function has been eliminated entirely.

The relationship in Eq. (A1) between the static structure function $S(q)$ and the particle-hole interaction $\tilde{V}_{\text{p-h}}(q)$ can also be derived from Eq. (1.7), if the Lindhard function is replaced with its "mean spherical" or "collective" approximation (CA),

$$\chi_0^{\mathrm{CA}}(q;\omega) = \frac{2t(q)}{(\hbar\omega + i\eta)^2 - t^2(q)/S_{\mathrm{F}}^2(q)}. \tag{A5}$$

The essence of this approximation is to replace the branch cut in $\chi_0(q;\omega)$ by a single pole; its strength chosen such that the first two sum rules agree when evaluated with the full Lindhard function $\chi_0(q;\omega)$ or in the collective approximation $\chi_0^{\mathrm{CA}}(q;\omega)$, i.e.,

$$\Im m\int d\omega\chi_0^{\mathrm{CA}}(q;\omega) = \Im m\int d\omega\chi_0(q;\omega),$$

$$\Im m\int d\omega\omega\chi_0^{\mathrm{CA}}(q;\omega) = \Im m\int d\omega\omega\chi_0(q;\omega). \tag{A6}$$

In fact, Eq. (1.7) together with Eq. (A5) or, alternatively,

$$\tilde{V}_{\text{p-h}}(q) = \frac{t(q)}{2}\left(\frac{1}{S^2(q)} - \frac{1}{S_{\mathrm{F}}^2(q)}\right) \tag{A7}$$

can be used[28] to *define* the particle-hole interaction from an accurately known $S(q)$.

The energy, consisting of kinetic and potential energies $\langle T\rangle+\langle V\rangle$, is[28]

$$E = \frac{3}{5}Nt_{\mathrm{F}} + E_{\mathrm{R}} + E_{\mathrm{Q}},$$

$$E_{\mathrm{R}} = \frac{\rho N}{2}\int d^3r\left\{g(r)v(r) + \frac{\hbar^2}{m}[1+C(r)]|\nabla\sqrt{1+\Gamma_{\mathrm{dd}}(r)}|^2\right\},$$

$$E_{\mathrm{Q}} = \frac{N}{4}\int\frac{d^3q}{(2\pi)^2\rho}t(q)\tilde{\Gamma}_{\mathrm{dd}}^2(q)[S_{\mathrm{F}}^2(q)/S(q) - 1]. \tag{A8}$$

Here, t_{F} is the Fermi energy of noninteracting particles, and, in this approximation,

$$\tilde{C}(q) = S_{\mathrm{F}}(q) - 1 + [S_{\mathrm{F}}^2(q) - 1]\tilde{\Gamma}_{\mathrm{dd}}(q). \tag{A9}$$

To make the connection with the limiting behavior of $\chi(q;0)$ in Sec. V C, we next spell out what is known as the uniform limit or CA. Products of functions which *in coordinate space* vanish for $r\to\infty$ are considered small. This implies to expand $\nabla\sqrt{1+\Gamma_{\mathrm{dd}}(r)}\approx\frac{1}{2}\nabla\Gamma_{\mathrm{dd}}(r)$ and to neglect $C(r)$. The kinetic energy then is

$$\langle T\rangle^{\mathrm{CA}} = T_{\mathrm{F}} + \frac{1}{4}\sum_{\mathbf{q}} t(q)S(q)\tilde{X}_{\mathrm{dd}}^2(q). \tag{A10}$$

Here, $T_{\mathrm{F}}=3Nt_{\mathrm{F}}/5$ and $\tilde{X}_{\mathrm{dd}}(q)$ is the "non-nodal" function. In our reduced FHNC approximation, $\tilde{X}_{\mathrm{dd}}(q)$ is related to the static structure factor by

$$\tilde{X}_{\mathrm{dd}}(q) = \frac{1}{S_{\mathrm{F}}(q)} - \frac{1}{S(q)}. \tag{A11}$$

APPENDIX B: DIAGRAMMATIC ANALYSIS

1. Transition density

We first examine the diagrammatic structure of CBF matrix elements $\rho_{0,ph}(\mathbf{r})$ of the density operator, Eqs. (3.10) and (3.11). The simplest approximation for $M_{ph,p'h'}$ has been spelled out in Eq. (4.6), the corresponding approximation for $\rho_{0,ph}(\mathbf{r})$ is

$$\rho_{0,ph}(\mathbf{r}) = \rho_{0,ph}^{\mathrm{F}}(\mathbf{r}) + \rho\int d^3r'\int d^3r''\left[\delta(\mathbf{r}-\mathbf{r}') - \frac{\rho}{\nu}\ell^2(|\mathbf{r}-\mathbf{r}'|k_{\mathrm{F}})\right]\Gamma_{\mathrm{dd}}(\mathbf{r}'-\mathbf{r}'')\rho_{0,ph}^{\mathrm{F}}(\mathbf{r}''). \tag{B1}$$

The diagrammatic representation of some leading diagrams contributing to $\rho_{0,ph}(\mathbf{r})$ is shown in Fig. 10. As usual, open points represent particle coordinates $\mathbf{r}_i$ while filled points indicate an integration over the associate coordinate

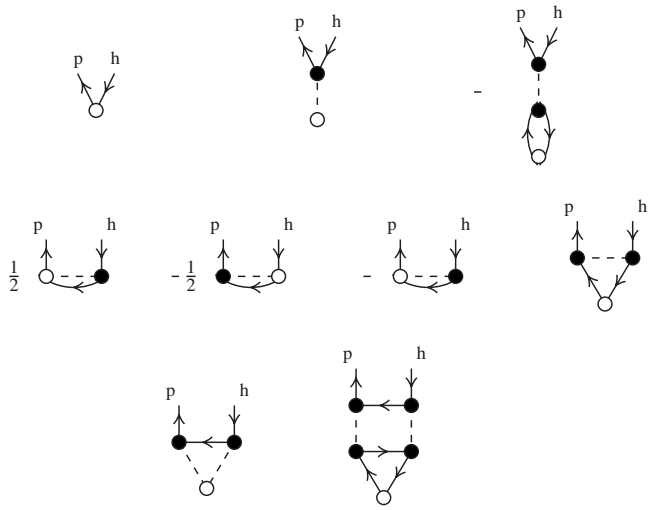

FIG. 10. Diagrammatic representation of some contributions to $\rho_{0,ph}(\mathbf{r})$. The upper row shows the diagrams defining the local approximation. The second row are the leading exchange diagrams and the third row shows two corrections due to the nonlocality of $\mathcal{N}(1,2)$.

space and a density factor. Dashed lines connecting points $\mathbf{r}_i$ and $\mathbf{r}_j$ represent a function $\Gamma_{\rm dd}(r_{ij})$ and oriented solid lines an exchange function $\ell(r_{ij}k_{\rm F})$. New elements are particle and hole states, depicted as upward (particles) or downward (holes) lines entering or leaving the diagram.

The three leading terms in Eq. (B2) are shown in the upper row of Fig. 10. In the second row of Fig. 10 we show the leading exchange diagrams. In the representation Eq. (3.10), these originate from the factors z_{ph} in the definition of the $\tilde{\rho}_{0,ph}(\mathbf{r})$, these are shown as the first two diagrams. Exchange terms also originate from the matrix element $\langle ph'|\Gamma_{\rm dd}|hp'\rangle_a$, these are shown as third and fourth diagrams in that row. Evidently there is a partial cancellation. The diagrams shown in that row also serve as an example for how the representations Eqs. (3.10) and (3.11) are equal. Starting from the form Eq. (3.11), the diagrams originating from the z_{ph} factors (i.e., the first two diagrams in the second row), have opposite signs; and the exchange term of $\langle pp'|\Gamma_{\rm dd}|hh'\rangle_a$ yields the third diagram with interchanged particle and hole labels. The sum of all three diagrams is the same.

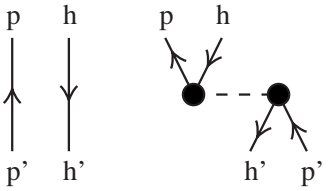

FIG. 11. Diagrammatic representation of the local approximation for $M_{ph,p'h'}$.

2. $M^{(\rm I)}$ matrix

Our next task is to show that the diagrams representing $M^{(\rm I)}_{ph,p'p''h'h''}$ are a proper subset of those contributing to $M_{ph,p'p''h'h''}$. We restrict ourselves here to the simplest case, which is the numerically implemented version. We start with the two-body matrix $M_{ph,p'h'}$. As spelled out in Eq. (4.6), besides the δ function, the leading contribution is the *local* term in the two-body operator

$$\mathcal{N}_{\rm loc}(1,2) = \Gamma_{\rm dd}(r_{12}). \tag{B2}$$

The diagrammatic representation of this approximation for $M_{ph,p'h'}$ is shown in Fig. 11.

A diagrammatic expansion of the matrix elements $M_{ph,p'p''h'h''}$ can be derived in exactly the same way as the corresponding expansions of the two-body matrix elements.[31] Generally, the $M_{ph,p'p''h'h''}$ are matrix elements of a nonlocal three-body operator, which can be expressed in terms of FHNC diagrams. Restricting ourselves again to the numerically implemented level, we need these quantities in an approximation equivalent to the uniform limit approximation[17] for bosons. We generalize this approach to fermions by keeping all diagrams contained in the Bose case plus those, where the end points of the correlation functions are linked by exchange paths [the bosonic $g(r_{ij})-1$ is identified with the direct-direct correlation function $\Gamma_{\rm dd}(r_{ij})$]. This procedure has already been used for deriving the optimal triplet correlations for the fermion ground state.[28] The diagrammatic representation of this approximation is shown in Fig. 12, the analytic form is

$$\begin{aligned} M^{\rm CA}_{ph,p'p''h'h''} = {} & \delta_{h,h'}\langle ph''|\Gamma_{\rm dd}(1,2)|p'p''\rangle - \delta_{p,p'}\langle h'h''|\Gamma_{\rm dd}(1,2)|hp''\rangle + \frac{1}{2}\langle ph'h''|\Gamma_{\rm dd}(3,1)\Gamma_{\rm dd}(1,2)|hp'p''\rangle \\ & - \frac{1}{2}\sum_{h_1}\langle ph''|\Gamma_{\rm dd}|h_1p''\rangle\langle h'h_1|\Gamma_{\rm dd}|p'h\rangle - \frac{1}{2}\sum_{h_1}\langle ph'|\Gamma_{\rm dd}|h_1p'\rangle\langle h''h_1|\Gamma_{\rm dd}|p''h\rangle + \langle ph'h''|\Gamma_{\rm dd}(1,2)\Gamma_{\rm dd}(2,3)|hp'p''\rangle \\ & - \sum_{h_1}\langle ph'|\Gamma_{\rm dd}|hh_1\rangle\langle h''h_1|\Gamma_{\rm dd}|p''p'\rangle - \sum_{h_1}\langle ph_1|\Gamma_{\rm dd}|hp'\rangle\langle h'h''|\Gamma_{\rm dd}|h_1p''\rangle + \langle ph'h''|\Gamma^{\rm CA}_{\rm ddd}(1,2,3)|hp'p''\rangle \\ & + \{(p'h') \leftrightarrow (p''h'')\}. \end{aligned} \tag{B3}$$

Here, in convolution approximation,

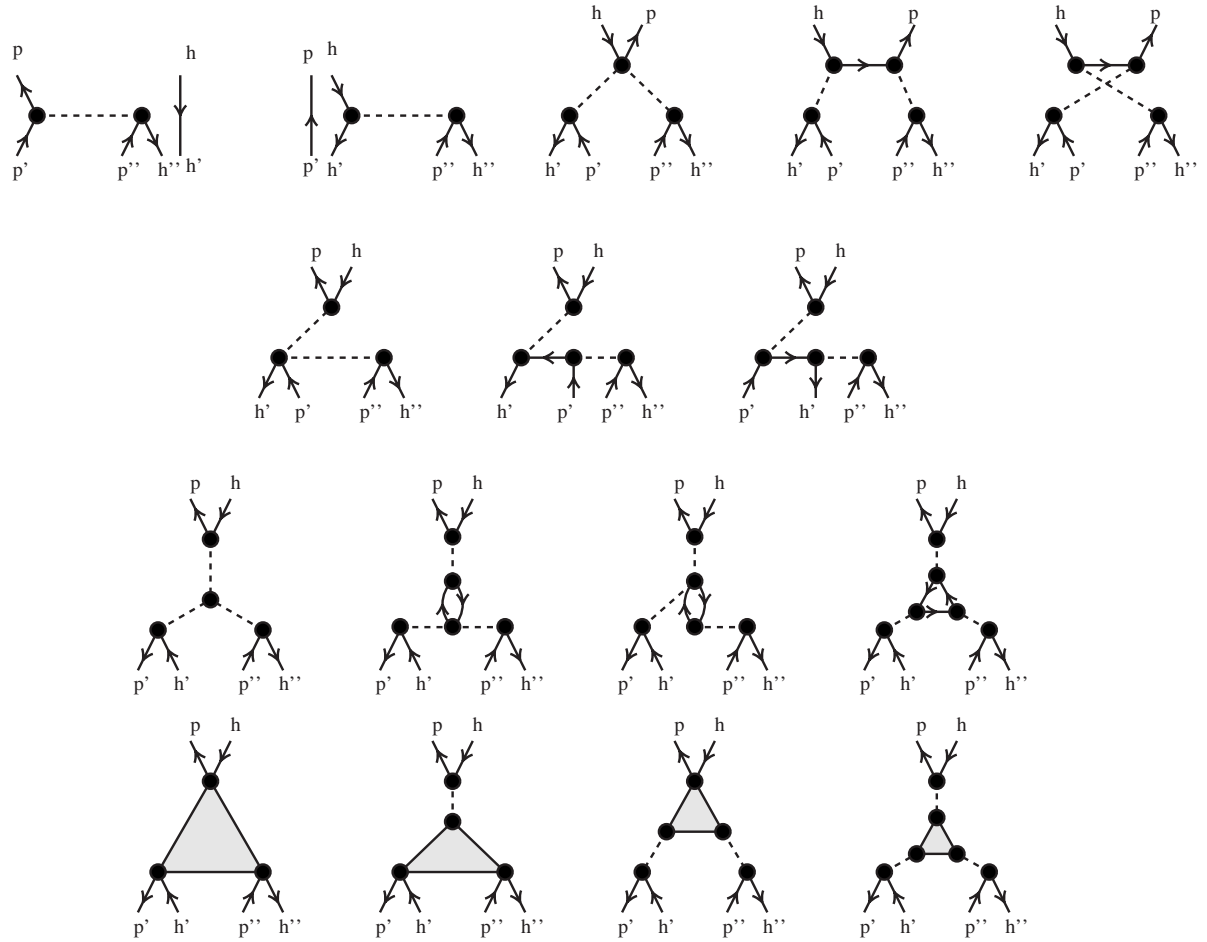

FIG. 12. Diagrams of $M_{ph,p'p''h'h''}$ in the convolution approximation Eq. (B3). Graphs obtained by exchanging the pairs $(p'h')$ and $(p''h'')$ are to be added. The last row shows some diagrams containing ground-state triplet correlations (shaded triangle), all of these contribute to $M^{(\mathrm{I})}_{ph,p'p''h'h''}$.

$$\Gamma^{\mathrm{CA}}_{\mathrm{ddd}}(\mathbf{r}_1,\mathbf{r}_2,\mathbf{r}_3) = \frac{\rho}{2}\int d^3r_4 \Gamma_{\mathrm{dd}}(\mathbf{r}_1-\mathbf{r}_4)\Gamma_{\mathrm{dd}}(\mathbf{r}_2-\mathbf{r}_4)\Gamma_{\mathrm{dd}}(\mathbf{r}_3-\mathbf{r}_4)$$
$$+\frac{\rho^2}{2\nu}\int d^3r_4 d^3r_5 \ell^2(|\mathbf{r}_4-\mathbf{r}_5|k_{\mathrm{F}})\Gamma_{\mathrm{dd}}(\mathbf{r}_1-\mathbf{r}_4)\Gamma_{\mathrm{dd}}(\mathbf{r}_2-\mathbf{r}_5)\Gamma_{\mathrm{dd}}(\mathbf{r}_3-\mathbf{r}_5)$$
$$+\frac{\rho^2}{\nu}\int d^3r_4 d^3r_5 \ell^2(|\mathbf{r}_4-\mathbf{r}_5|k_{\mathrm{F}})\Gamma_{\mathrm{dd}}(\mathbf{r}_1-\mathbf{r}_4)\Gamma_{\mathrm{dd}}(\mathbf{r}_3-\mathbf{r}_4)\Gamma_{\mathrm{dd}}(\mathbf{r}_2-\mathbf{r}_5)$$
$$+\frac{\rho^3}{\nu^2}\int d^3r_4 d^3r_5 d^3r_6 \ell(|\mathbf{r}_4-\mathbf{r}_5|k_{\mathrm{F}})\ell(|\mathbf{r}_5-\mathbf{r}_6|k_{\mathrm{F}})\ell(|\mathbf{r}_6-\mathbf{r}_4|k_{\mathrm{F}})\Gamma_{\mathrm{dd}}(\mathbf{r}_1-\mathbf{r}_4)\Gamma_{\mathrm{dd}}(\mathbf{r}_2-\mathbf{r}_5)\Gamma_{\mathrm{dd}}(\mathbf{r}_3-\mathbf{r}_6). \quad \text{(B4)}$$

The first two lines are invariant under exchanging $\mathbf{r}_2 \leftrightarrow \mathbf{r}_3$, equivalent to exchanging $(p'h') \leftrightarrow (p''h'')$ in Eq. (B3).

Optimized triplet correlations improve the description of the ground-state structure, in particular, in the area of the peak of the static structure function and also improve, for bosons, the density dependence of the spectrum.[17] These correlations add another term to the three-body function $\Gamma^{\mathrm{CA}}_{\mathrm{ddd}}(\mathbf{r}_1,\mathbf{r}_2,\mathbf{r}_3)$. The expressions are lengthy,[28] we refrain from spelling them out here and just show the diagrammatic representation of some typical terms in the last row of Fig. 12.

Per definition in Eq. (3.16), $M^{(\mathrm{I})}_{ph,p'p''h'h''}$ is to be constructed such that its matrix product with $M_{ph,p'h'}$ reproduces $M_{ph,p'p''h'h''}$. A low-order manifestation of this is easily verified with choosing for $M^{(\mathrm{I})}_{ph,p'p''h'h''}$ the uniform limit diagrams shown in the first row of Fig. 12,

$$M^{(\mathrm{I})\mathrm{CA}}_{ph,p'p''h'h''} = \{\delta_{h,h'}\langle ph''|\Gamma_{\mathrm{dd}}|p'p''\rangle - \delta_{p,p'}\langle h'h''|\Gamma_{\mathrm{dd}}|hp''\rangle + (p'h') \leftrightarrow (p''h'')\}$$
$$+ \sum_{p_1}\langle ph''|\Gamma_{\mathrm{dd}}|p_1p''\rangle\langle p_1h'|\Gamma_{\mathrm{dd}}|hp'\rangle - \sum_{h_1}\langle ph'|\Gamma_{\mathrm{dd}}|h_1p'\rangle\langle h_1h''|\Gamma_{\mathrm{dd}}|hp''\rangle, \tag{B5}$$

$$= \frac{1}{N}\delta_{\mathbf{q},\mathbf{q}'+\mathbf{q}''}\bar{n}_{\mathbf{p}}\bar{n}_{\mathbf{p}'}\bar{n}_{\mathbf{p}''}n_{\mathbf{h}}n_{\mathbf{h}'}n_{\mathbf{h}''}\left[\{\tilde{\Gamma}_{\mathrm{dd}}(q'')(\delta_{h,h'} - \delta_{p,p'}) + (p'h') \leftrightarrow (p''h'')\} + \frac{1}{N}\tilde{\Gamma}_{\mathrm{dd}}(q'')\tilde{\Gamma}_{\mathrm{dd}}(q')(\bar{n}_{\mathbf{h}+\mathbf{q}'} - n_{\mathbf{h}+\mathbf{q}''})\right], \tag{B6}$$

where the term originating from triplet correlations has not been spelled out.

Generally, $M^{(\mathrm{I})}_{ph,p'p''h'h''}$ is represented by the subset of $M_{ph,p'p''h'h''}$ diagrams that cannot be cut into two pieces, one connected to the labels ph and the other to $p'p''h'h''$, by cutting either two exchange lines or cutting the diagram in an internal point.The third row of Fig. 12 shows such contributions.

$M^{(\mathrm{I})\mathrm{CA}}_{ph,p'p''h'h''}$ depends nontrivially on three-particle and three-hole quantum numbers. We define the localized version as its Fermi sea average, Eq. (4.5),

$$\tilde{M}^{(\mathrm{I})\mathrm{CA}}_{q,q'q''} \equiv \frac{1}{S_{\mathrm{F}}(q)S_{\mathrm{F}}(q')S_{\mathrm{F}}(q'')}\frac{1}{N}\sum_{hh'h''} M^{(\mathrm{I})\mathrm{CA}}_{ph,p'p''h'h''}$$
$$= \delta_{\mathbf{q},\mathbf{q}'+\mathbf{q}''}\left\{\left[\frac{S(q')S(q'')}{S_{\mathrm{F}}(q')S_{\mathrm{F}}(q'')} - 1\right]\frac{S^{(3)}_{\mathrm{F}}(q,q',q'')}{S_{\mathrm{F}}(q)S_{\mathrm{F}}(q')S_{\mathrm{F}}(q'')}\right.$$
$$\left. + \frac{S(q')S(q'')}{S_{\mathrm{F}}(q')S_{\mathrm{F}}(q'')}\tilde{u}_3(q,q',q'')\right\}. \tag{B7}$$

Here, the relationship in Eq. (A4) was used for the connection between $\tilde{\Gamma}_{\mathrm{dd}}(q)$ and $S(q)$ and

$$S^{(3)}_{\mathrm{F}}(q,q',q'') \equiv \frac{1}{N}\sum_{h} n_{\mathbf{h}}\bar{n}_{\mathbf{h}-\mathbf{q}}[\bar{n}_{\mathbf{h}+\mathbf{q}'} - n_{\mathbf{h}+\mathbf{q}''}] \tag{B8}$$

is the three-body static structure function of noninteracting fermions.

3. Three-body vertices

We now apply the localization procedure Eq. (4.5) to the three-body vertices. Starting with Eq. (3.35), we have

$$\tilde{K}^{(q)}_{q'q'',0} \equiv N^2K^{(q)}_{q'q'',0} = \frac{1}{NS_{\mathrm{F}}(q)S_{\mathrm{F}}(q')S_{\mathrm{F}}(q'')}\sum_{hh'h''}\left[H'_{pp'p''hh'h'',0}\right.$$
$$\left. - \sum_{p_1h_1} H'_{pp_1hh_1,0}M^{(\mathrm{I})}_{p'p''h'h'',p_1h_1}\right]. \tag{B9}$$

As discussed in Sec. III B, the Euler Eq. (2.5) for the ground-state optimizations ensure that the Fermi sea average Eq. (3.7) of $H'_{pp'p''hh'h'',0}$ vanishes. For the matrix elements $H'_{pp_1hh_1,0}$ Eqs. (4.1)–(4.3) yield

$$H'_{pp_1hh_1,0} = \frac{1}{2N}\delta_{\mathbf{q}+\mathbf{q}',\mathbf{0}}\left[e_{ph} + e_{p'h'} - 2\frac{t(q)}{S_{\mathrm{F}}(q)}\right]\tilde{\Gamma}_{\mathrm{dd}}(q). \tag{B10}$$

Therefore, using Eq. (B6) for $M^{(\mathrm{I})}_{ph,p'p''h'h''}$

$$\frac{1}{N^3}\sum_{hh'h''} K^{(ph)}_{p'p''h'h'',0} = -\frac{1}{N^3}\sum_{hh'h''}\sum_{p_1h_1} H'_{pp_1hh_1,0}M^{(\mathrm{I})}_{p'p''h'h'',p_1h_1}$$
$$= -\frac{1}{2N^3}\tilde{\Gamma}_{\mathrm{dd}}(q)S_{\mathrm{F}}(q)\sum_{h'h''h_1}\left[e_{h_1-q,h_1}\right.$$
$$\left. - \frac{t(q)}{S_{\mathrm{F}}(q)}\right]M^{(\mathrm{I})}_{p'p''h'h'',(h_1-q)h_1}$$
$$= \frac{\delta_{\mathbf{q}+\mathbf{q}'+\mathbf{q}'',0}}{N^2}\frac{\hbar^2}{4m}\tilde{\Gamma}_{\mathrm{dd}}(q)\left[\frac{S(q')S(q'')}{S_{\mathrm{F}}(q')S_{\mathrm{F}}(q'')} - 1\right]$$
$$\times\{q^2S^{(3)}_{\mathrm{F}}(q,q',q'')$$
$$+ \mathbf{q}\cdot[\mathbf{q}''S_{\mathrm{F}}(q') + \mathbf{q}'S_{\mathrm{F}}(q'')]S_{\mathrm{F}}(q)\}. \tag{B11}$$

This term vanishes when q and q' are larger than $2k_{\mathrm{F}}$. It is also zero if the matrix element $H'_{pp_1hh_1,0}$ in Eq. (B11) is replaced by its Fermi sea average. We therefore expect this term to be small, in particular, since it has no analog in the Bose limit. Note also that triplet ground-state correlations do not contribute to this term. Dividing by the normalization factors $S_{\mathrm{F}}(q)S_{\mathrm{F}}(q')S_{\mathrm{F}}(q'')$ leads to the result in Eq. (4.13).

To calculate a localized version of the vertex $K_{ph,p'p''h'h''}$, Eq. (3.34), we need

$$\tilde{K}_{q,q'q''} \equiv N^2K_{q,q'q''} = \frac{1}{NS_{\mathrm{F}}(q)S_{\mathrm{F}}(q')S_{\mathrm{F}}(q'')}\sum_{hh'h''}\left[H'_{ph,p'p''h'h''}\right.$$
$$\left. - \sum_{p_1h_1} H'_{ph,p_1h_1}M^{(\mathrm{I})}_{p_1h_1,p'p''h'h''}\right] \tag{B12}$$

with

$$H'_{ph,p'h'} = \delta_{\mathbf{q},\mathbf{q}'}\left\{\delta_{h,h'}e_{ph} + \frac{1}{2N}\left[e_{ph} + e_{p'h'} - 2\frac{t(q)}{S_{\mathrm{F}}(q)}\right]\tilde{\Gamma}_{\mathrm{dd}}(q)\right\}. \tag{B13}$$

We first separate the contribution that survives in the boson limit. Starting with the identity

$$\sum_{h'h''} |\Psi_{p'p''h'h''}\rangle = F\left[\hat{\rho}_{\mathbf{q}'}\hat{\rho}_{\mathbf{q}''} - \sum_{h'} a^{\dagger}_{h'+q'+q''}a_{h'}(\bar{n}_{\mathbf{h}'+\mathbf{q}''} - n_{\mathbf{h}'+\mathbf{q}'})\right]|\Phi_{\mathbf{o}}\rangle \tag{B14}$$

we have

$$\sum_{hh'h'} H'_{ph,p'p''h'h''} = \langle\Psi_{\mathbf{o}}|\hat{\rho}_{\mathbf{q}}H'\hat{\rho}_{\mathbf{q}'}\hat{\rho}_{\mathbf{q}''}|\Psi_{\mathbf{o}}\rangle - \sum_{hh'}(\bar{n}_{\mathbf{h}'+\mathbf{q}''} - n_{\mathbf{h}'+\mathbf{q}'})H_{ph,h'+qh'}. \tag{B15}$$

Postulating that three-body correlations have been optimized we can simplify the first term

$$\frac{1}{2N}\langle\Psi_{\mathbf{o}}|[[\hat{\rho}_{\mathbf{q}},H'],\hat{\rho}_{\mathbf{q}'}\hat{\rho}_{\mathbf{q}''}]|\Psi_{\mathbf{o}}\rangle = -\frac{\hbar^2}{2m}\mathbf{q}\cdot[\mathbf{q}''S(q') + \mathbf{q}'S(q'')]. \tag{B16}$$

For the form Eq. (B13), the second term in Eq. (B15) is

$$-\frac{1}{N}\sum_{hh'} H_{ph,h'+qh'}(\bar{n}_{\mathbf{h}'+\mathbf{q}''} - n_{\mathbf{h}'+\mathbf{q}'}) = \frac{\hbar^2}{2m}\mathbf{q}\cdot[\mathbf{q}''S_{\mathrm{F}}(q') + \mathbf{q}'S_{\mathrm{F}}(q'')] + \frac{\hbar^2}{4m}\tilde{\Gamma}_{\mathrm{dd}}(q)[q^2S^{(3)}_{\mathrm{F}}(q,q',q'') + \mathbf{q}\cdot[\mathbf{q}''S_{\mathrm{F}}(q') + \mathbf{q}'S_{\mathrm{F}}(q'')]S_{\mathrm{F}}(q)]. \tag{B17}$$

The remaining term of $\tilde{K}_{q,q'q''}$ in Eq. (3.35), $-\Sigma_{p_1h_1}H'_{ph,p_1h_1}M^{(\mathrm{I})}_{p_1h_1,p'p''h'h''}$, contains contributions originating from the diagonal and the off-diagonal parts of H'_{ph,p_1h_1}, Eq. (B13). The off-diagonal part is identical to expression (B11) whereas the contribution from the diagonal term gives

$$-\frac{1}{N}\sum_{h,h',h''} e_{ph}M^{(\mathrm{I})}_{ph,p'p''h'h''} = \frac{\hbar^2}{2m}\mathbf{q}\cdot[\mathbf{q}''S_{\mathrm{F}}(q') + \mathbf{q}'S_{\mathrm{F}}(q'')]\times\left[\frac{S(q')S(q'')}{S_{\mathrm{F}}(q')S_{\mathrm{F}}(q'')} - 1\right] - \frac{\hbar^2q^2}{2m}S(q')S(q'')\tilde{u}_3(q,q',q''). \tag{B18}$$

Collecting the individual contributions we obtain Eq. (4.12).

4. Four-body coupling matrix element

In Eq. (3.24) we have defined the irreducible four-body coupling matrix element $M^{(\mathrm{I})}_{pp'hh',p''p'''h''h'''}$. Again, "irreducible" means that in the diagrammatic representation left and right arguments cannot be separated by cutting a particle and a hole line. In analogy to the Bose case the "convolution" (uniform limit) approximation is obtained by retaining the leading-order diagrams

$$M^{(\mathrm{I})\mathrm{CA}}_{pp'hh',p''p'''h''h'''} \equiv M_{ph,p''h''}M_{p'h',p'''h'''} + M_{ph,p'''h'''}M_{p'h',p''h''}. \tag{B19}$$

This contains all diagrams with up to two correlations. A consistent improvement of the convolution approximation involves an infinite resummation. For bosons[7] this had only a marginal effect. We expect a similarly small improvement for fermions.

The approximation for $K_{pp'hh',p''p'''h''h'''}$ consistent with Eq. (B19) is to keep all diagrams containing only one correlation function $\Gamma_{\mathrm{dd}}(r)$,

$$K^{\mathrm{CA}}_{pp'hh',p''p'''h''h'''} \equiv \delta_{p,p''}\delta_{h,h''}e_{ph}M_{p'h',p'''h'''} + \delta_{p',p'''}\delta_{h',h'''}e_{p'h'}M_{ph,p''h''} + \{p''h'' \leftrightarrow p'''h'''\}. \tag{B20}$$

Note that both $M^{(\mathrm{I})\mathrm{CA}}_{pp'hh',p''p'''h''h'''}$ and $K^{\mathrm{CA}}_{pp'hh',p''p'''h''h'''}$ contain explicit particle and hole labels. Again, we no longer spell out the superscript "CA" in the following.

A word is in order about the symmetry of both quantities. Equations (B19) and (B20) show that both operators are the sum of two term that differ from each other merely by the interchanging $\{p''h'' \leftrightarrow p'''h'''\}$. We have discussed in connection with Eq. (3.42) that it is legitimate to replace $M^{(\mathrm{I})}_{pp'hh',p''p'''h''h'''}$ and $K_{pp'hh',p''p'''h''h'''}$ by their asymmetric form.

APPENDIX C: PAIR PROPAGATOR

1. Pair-energy matrix

A priori, $E_{pp'hh',p''p'''h''h'''}(\omega)$ is a function of four-hole and four-particle momenta as well as the energy. In the uniform limit approximation we can, however, express the inverse in terms of two-body quantities. From Eqs. (B19) and (B20) we obtain the pair-energy matrix

$$E_{pp'hh',p''p'''h''h'''}(\omega) = (\hbar\omega + i\eta)M_{ph,p''h''}M_{p'h',p'''h'''} - (\delta_{p,p''}\delta_{h,h''}e_{ph})M_{p'h',p'''h'''} - M_{ph,p''h''}(\delta_{p',p'''}\delta_{h',h'''}e_{p'h'}). \tag{C1}$$

To calculate its inverse, write Eq. (C1) as

$$\sum_{p_1h_1p_2h_2} M^{-1}_{ph,p_1h_1}M^{-1}_{p'h',p_2h_2}E_{p_1p_2h_1h_2,p''p'''h''h'''}(\omega) = (\hbar\omega + i\eta)\delta_{p,p''}\delta_{h,h''}\delta_{p',p'''}\delta_{h,h'''} - (M^{-1}_{ph,p''h''}e_{p''h''})\delta_{p',p'''}\delta_{h,h'''} - \delta_{p,p''}\delta_{h,h''}(M^{-1}_{p'h',p'''h'''}e_{p'''h'''}). \tag{C2}$$

Use now, for two commuting operators A,B

$$[(\hbar\omega + i\eta) - \mathrm{A} - \mathrm{B}]^{-1}$$
$$= -\int_{-\infty}^{\infty} \frac{d(\hbar\omega')}{2\pi i}[(\hbar\omega' + i\eta) - \mathrm{A}]^{-1}[\hbar(\omega - \omega' + i\eta) - \mathrm{B}]^{-1}, \tag{C3}$$

which can be proved by series expansion. Consequently, we have

$$E^{-1}_{pp'hh',p''p'''h''h'''}(\omega) = -\int_{-\infty}^{\infty} \frac{d(\hbar\omega')}{2\pi i} \kappa_{ph,p''h''}(\omega') \times \kappa_{p'h',p'''h'''}(\omega - \omega') \tag{C4}$$

with

$$\kappa_{ph,p'h'}(\omega) \equiv [(\hbar\omega + i\eta)M_{ph,p'h'} - \delta_{pp'}\delta_{hh'}e_{ph}]^{-1}. \tag{C5}$$

For our choice Eq. (4.6) of $M_{p'h',ph}$, we can calculate $\kappa_{ph,p'h'}(\omega)$ analytically,

$$\kappa_{ph,p'h'}(\omega) = \frac{\delta_{p,p'}\delta_{h,h'}}{\hbar\omega - e_{ph} + i\eta} - \frac{1}{\hbar\omega - e_{ph} + i\eta} \frac{\hbar\omega\tilde{\Gamma}_{\mathrm{dd}}(q)/N}{1 + \hbar\omega\tilde{\Gamma}_{\mathrm{dd}}(q)\kappa^0(q;\omega)} \times \frac{1}{\hbar\omega - e_{p'h'} + i\eta}, \tag{C6}$$

where $\kappa^0(q;\omega)$ has been defined in Eq. (5.5).

According to Eqs. (3.43) and (4.14), the dynamic parts of the interactions are obtained from matrix products of $E^{-1}_{pp'hh',p''p'''h''h'''}(\omega)$ as given in Eq. (C4) with the three-body vertices in Eqs. (4.12) and (4.13). The latter being local functions, only sums over the hole states enter $V_{\mathrm{A,B}}(q;\omega)$.

$$\tilde{E}^{-1}(q_1,q_2;\omega) \equiv \frac{1}{N^2}\sum_{h_1h_2h_1'h_2'} E^{-1}_{p_1p_2h_1h_2,p_1'p_2'h_1'h_2'}(\omega) = -\int_{-\infty}^{\infty} \frac{d(\hbar\omega')}{2\pi i}\kappa(q_1;\omega')\kappa(q_2;\omega - \omega') \tag{C7}$$

with

$$\kappa(q;\omega) \equiv \frac{1}{N}\sum_{hh'} \kappa_{ph,p'h'}(\omega) = \frac{\kappa_0(q;\omega)}{1 + \hbar\omega\tilde{\Gamma}_{\mathrm{dd}}(q)\kappa_0(q;\omega)}. \tag{C8}$$

Using Kramers-Kronig relations, we obtain the useful alternative representation

$$\tilde{E}^{-1}(q_1,q_2;\omega) = \int_{-\infty}^{\infty} \frac{d(\hbar\omega_1)d(\hbar\omega_2)}{\pi^2} \frac{\Im m\kappa(q_1;\omega_1)\Im m\kappa(q_2;\omega_2)}{\hbar\omega_1 + \hbar\omega_2 - \hbar\omega - i\eta}. \tag{C9}$$

2. Properties of the pair propagator

a. Properties of $\kappa(q;\omega)$

The structure of $\kappa(q;\omega)$ resembles that of $\chi(q;\omega)$ in the RPA. It features a particle-hole continuum $\kappa_{\mathrm{cont}}(q;\omega)$, and, possibly, a "collective mode" with a dispersion relation given by

$$1 + \kappa_0(q;\omega_{\mathrm{c}}(q))\hbar\omega_{\mathrm{c}}(q)\tilde{\Gamma}_{\mathrm{dd}}(q) = 0. \tag{C10}$$

We can therefore write

$$\Im m\kappa(q,\omega) = z(q)\pi\delta(\hbar\omega - \hbar\omega_{\mathrm{c}}(q)) + \Im m\kappa_{\mathrm{cont}}(q;\omega),$$
$$z(q) = \left.\frac{\kappa_0(q;\omega)}{\tilde{\Gamma}_{\mathrm{dd}}(q)\dfrac{d}{d\omega}\omega\kappa_0(q;\omega)}\right|_{\omega_{\mathrm{c}}(q)}. \tag{C11}$$

$\kappa(q;\omega)$ satisfies the following sum rules which we write in the suggestive way:

$$\frac{S^2(q)}{S_{\mathrm{F}}^2(q)}\int_0^{\infty} \frac{d(\hbar\omega)}{\pi}\Im m\kappa(q;\omega) = -S(q), \tag{C12}$$

$$\frac{S^2(q)}{S_{\mathrm{F}}^2(q)}\int_0^{\infty} \frac{d(\hbar\omega)}{\pi}\hbar\omega\Im m\kappa(q;\omega) = -t(q). \tag{C13}$$

Equation (C12) is proved by extending the integration to $-\infty$, noting that $\kappa_0(q;\omega)$ is real on the negative ω axis. Since $\kappa_0(q;\omega)$ has no poles in the upper complex plane, we can evaluate the integral along a circle, using the asymptotic expansion

$$\kappa_0(q;\omega\to\infty) = \frac{S_{\mathrm{F}}(q)}{\hbar\omega} + \frac{t(q)}{\hbar^2\omega^2} + \mathcal{O}(\hbar\omega)^{-3}. \tag{C14}$$

The proof of Eq. (C13) proceeds along the same line, subtracting the asymptotic expansion of $\kappa(q;\omega)$ beforehand. From Eqs. (C12) and (C13) it is clear that the analytic properties of $S^2(q)\kappa(q;\omega)/S_{\mathrm{F}}^2(q)$ are similar to those of the density-density response function $\chi^{\mathrm{RPA}}(q;\omega)$. For bosons, the two functions coincide exactly: Identifying $\tilde{\Gamma}_{\mathrm{dd}}(q) = S(q) - 1$ and $S_{\mathrm{F}}(q) = 1$, $\kappa^0(q;\omega)$ consists of a single mode so that

$$\kappa_0(q;\omega) = \frac{1}{\hbar\omega + i\eta - t(q)},$$
$$\kappa(q;\omega) = \frac{1}{S(q)}\frac{1}{\hbar\omega + i\eta - \varepsilon(q)}. \tag{C15}$$

Figure 13 further confirms this similarity for ^{3}He at saturation density. Expectedly, a solution of Eq. (C10) is found to lie within a few percent of the RPA zero sound mode.

b. Properties of $\tilde{E}^{-1}(q,q';\omega)$

Equations (C12) and (C13) lead to the sum rules for the pair propagator,

$$\int_{-\infty}^{\infty} \frac{d(\hbar\omega)}{\pi}\Im mE^{-1}(q,q';\omega) = -\frac{S_{\mathrm{F}}^2(q)}{S(q)}\frac{S_{\mathrm{F}}^2(q')}{S(q')}, \tag{C16}$$

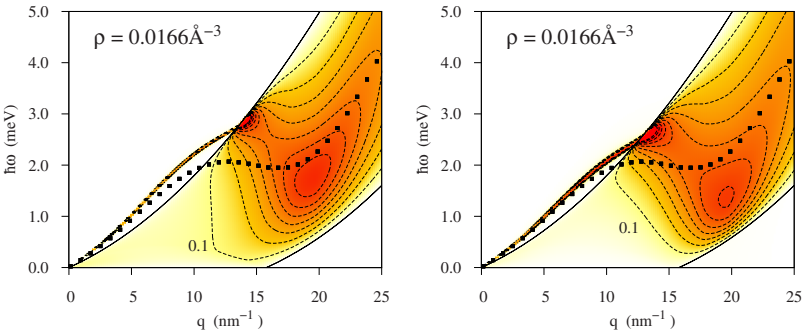

FIG. 13. (Color online) Imaginary part of the scaled propagator $S^2(q)\kappa(q,\omega)/S_F^2(q)$ (left) and of $\chi^{\mathrm{RPA}}(q,\omega)$ (right) at the density $\rho=0.0166$ Å^{-3}. The black squares show, for reference, the Feynman dispersion relation $\varepsilon(q)$. Dashed lines are equidistant contours at $0.1, 0.2, \ldots, 1.0 t_F^{-1}$.

$$\int_{-\infty}^{\infty} \frac{d(\hbar\omega)}{\pi} \hbar\omega \Im m E^{-1}(q,q';\omega) = -\frac{S_F^2(q)}{S(q)} \frac{S_F^2(q')}{S(q')} [\varepsilon(q)+\varepsilon(q')]. \tag{C17}$$

The proof of Eq. (C16) is best carried out starting from the representation Eq. (C9),

$$\int_0^{\infty} \frac{d(\hbar\omega)}{\pi} \Im m E^{-1}(q_1,q_2;\omega) = -\int_0^{\infty} \frac{d(\hbar\omega_1)}{\pi} \Im m \kappa(q_1;\omega_1) \times \int_0^{\infty} \frac{d(\hbar\omega)}{\pi} \Im m \kappa(q_2;\omega-\omega_1). \tag{C18}$$

The $\hbar\omega$ integral in the last term can be extended to $-\infty$ since $\Im m\kappa(q;\omega)$ is real on the negative ω axis.

If Eq. (C10) has a solution, the pair propagator has a collective mode. From Eq. (C11) we obtain

$$\Im m \tilde{E}^{-1}(q_1,q_2;\omega) = \pi z(q_1) z(q_2) \delta(\hbar\omega_c(q_1)+\hbar\omega_c(q_2)-\hbar\omega). \tag{C19}$$

This is the origin of two-phonon excitations or the double plasmon in charged systems.

The two-particle-two-hole band consists of three parts which may overlap. The first one is the continuum-continuum (c-c) coupling, where the contribution of each $\kappa(q;\omega)$ in Eq. (C7) comes from its particle-hole band. This defines the two-particle-two-hole "tube" in $(q,q';\omega)$ space. Its boundaries are

$$e_{\min}(q)+e_{\min}(q') \le \hbar\omega \le e_{\max}(q)+e_{\max}(q'), \tag{C20}$$

where $e_{\min}$ and $e_{\max}$ denote the upper and lower borders of each single-particle-hole band, respectively.

The other two parts of $E^{-1}(q,q';\omega)$ arise from continuum-mode (c-m) coupling, they are identical apart from interchanging q and q'. Their boundaries are

$$e_{\min}(q)+\hbar\omega_{\text{c-m}}(q') \le \hbar\omega \le e_{\max}(q)+\hbar\omega_{\text{c-m}}(q'). \tag{C21}$$

Finally, we consider three limits of the pair propagator. First, in the noninteracting case, $\tilde{\Gamma}_{\mathrm{dd}}(q)=0$, we simply obtain a sum over two-pair-energy denominators

$$\tilde{E}_F^{-1}(q,q';\omega) = -\int \frac{d(\hbar\omega')}{2\pi i} \kappa_0(q';\omega-\omega')\kappa_0(q;\omega') = \frac{1}{N^2}\sum_{hh'} \frac{1}{\hbar\omega+i\eta-e_{ph}-e_{p'h'}}, \tag{C22}$$

i.e., the two-particle energy denominator appropriate for perturbation theory in a weakly interacting Fermi system.

Second, Eq. (C15) reproduces the energy denominator appearing in the boson theory,

$$\tilde{E}_{\mathrm{bos}}^{-1}(q,q';\omega) = \frac{1}{S(q)S(q')} \frac{1}{\hbar\omega+i\eta-\varepsilon(q)-\varepsilon(q')}. \tag{C23}$$

Finally, we consider the collective or uniform limit approximation. Following Eq. (A6) we replace $\kappa_0(q;\omega)$ by that single-pole approximation which ensures its correct ω^0 and ω^1 sum rules. This gives

$$\kappa_0^{\mathrm{CA}}(q;\omega) = \frac{S_F(q)}{\hbar\omega+i\eta-t(q)/S_F(q)}, \tag{C24}$$

$$\kappa^{\mathrm{CA}}(q;\omega) = \frac{S_F^2(q)}{S(q)} \frac{1}{\hbar\omega+i\eta-\varepsilon(q)}, \tag{C25}$$

and

$$E_{\mathrm{CA}}^{-1}(q,q';\omega) = \frac{S_F^2(q)}{S(q)} \frac{S_F^2(q')}{S(q')} \frac{1}{\hbar\omega+i\eta-\varepsilon(q)-\varepsilon(q')}. \tag{C26}$$

The boson limit as well as the collective approximation demonstrate the effect of correlations. The single-particle energies get shifted and form a band around the "Feynman-spectrum." Note that the collective approximation satisfies the sum rules in Eqs. (C16) and (C17) exactly.

3. Pair propagator for charged systems

For charged systems, the dispersion of the solution of Eq. (C10) has, unlike the plasmon, a term that is linear in the wave number

$$\hbar\omega_c(q) = \omega_p + \frac{t_F}{6}\frac{q}{k_F} - \frac{9t_F^2}{4\hbar\omega_p}\left(\frac{q}{k_F}\right)^2 + \mathcal{O}(q^3). \tag{C27}$$

For the strength of this mode we obtain

$$z(q) = \frac{9\hbar\omega_p}{16t_F} - \frac{3}{32}\frac{q}{k_F}. \tag{C28}$$

Hence, to leading order, for the pole of $E^{-1}(q_1,q_2;\omega)$ in Eq. (C19) we obtain

$$\Im m\tilde{E}^{-1}(q',q';\omega) = -\pi\left(\frac{9}{16}\frac{\hbar\omega_p}{t_F} - \frac{3}{32}\frac{q'}{k_F}\right)^2 \times \delta\left(\hbar\omega - 2\hbar\omega_p - \frac{t_F}{3}\frac{q'}{k_F}\right) \quad \text{as} \quad q' \to 0. \tag{C29}$$

Note that the location of double-plasmon pole contains, in leading order in the momentum transfer, no information on many-body correlations.

APPENDIX D: LARGE MOMENTUM LIMIT

For large momenta, $S(q)-1$ falls off at least as q^{-4}. The vertices in Eqs. (4.12) and (4.13) fall off as q^{-1} and q^{-2}, respectively, hence we have

$$\tilde{K}_{q,q'q''} \approx \frac{S(q')S(q'')}{S_F(q')S_F(q'')}\frac{\hbar^2}{2m}[\mathbf{q}\cdot\mathbf{q}'\tilde{X}_{dd}(q') + \mathbf{q}\cdot\mathbf{q}''\tilde{X}_{dd}(q'')],$$

$$\tilde{K}^{(q)}_{q'q'',0} \approx 0. \tag{D1}$$

As a consequence, $\tilde{W}_B(q;0)$ is negligible for large momenta, and only the first term in Eq. (4.17) contributes to $\tilde{W}_A(q;0)$.

For large q either q' or q'' (or both) must be large (let $q'' \geq q'$, the symmetry in $\mathbf{q}' \leftrightarrow \mathbf{q}''$ just yielding a factor of 2). Since $\tilde{X}_{dd}(q)$ falls off for large q, the dominant contribution of Eq. (D1) then arises from small q' and we can write

$$\tilde{W}_A(q\to\infty;0) = \left(\frac{\hbar^2}{2m}\right)^2 \frac{1}{N}\sum_{\mathbf{q}'}\left(\frac{S(q')}{S_F(q')}\right)^2 [\mathbf{q}\cdot\mathbf{q}'\tilde{X}_{dd}(q')]^2 \times \tilde{E}^{-1}(q',q'';0)$$

$$= \frac{t(q)}{3}\frac{1}{N}\sum_{\mathbf{q}'} t(q')\left[\frac{S(q')}{S_F(q')}\tilde{X}_{dd}(q')\right]^2 \tilde{E}^{-1}(q',q;0). \tag{D2}$$

We now use the representation Eq. (C7) for the pair propagator

$$\tilde{E}^{-1}(q',q;0) = -\int_{-\infty}^{\infty}\frac{d\hbar\omega'}{\pi}\Re e\kappa(q';\omega')\Im m\kappa(q;-\omega'). \tag{D3}$$

Since $\kappa^0(q \gg k_F;\omega) = 1/[\hbar\omega - t(q) + i\eta]$ we have

$$\kappa(q\to\infty;\omega) = \frac{1}{S(q)}\frac{1}{\hbar\omega - \varepsilon(q) + i\eta}. \tag{D4}$$

Consequently,

$$\tilde{E}^{-1}(q',q\to\infty;0) = \frac{1}{S(q)}\Re e\kappa\left(q',-\frac{1}{\hbar}\varepsilon(q)\right) = -\frac{1}{t(q)}\frac{S_F^2(q')}{S(q')}, \tag{D5}$$

where the last equality follows from the high-frequency limit $\kappa^0(q';\omega) \to S_F(q')/\omega$. Insertion into Eq. (D2). yields

$$\tilde{W}_A(q\to\infty,0) = -\frac{1}{3N}\sum_{\mathbf{q}'} t(q')S(q')[\tilde{X}_{dd}(q')]^2, \tag{D6}$$

which together with Eq. (A10) gives the result in Eq. (5.15).

APPENDIX E: SUM RULES

For bosons, the ω^0 and ω^1 sum rules in Eqs. (1.4) and (1.5) are satisfied exactly[16] in the sense that the result of the frequency integration is independent of the level at which pair fluctuations are treated. This feature provides an unambiguous method to determine the static particle-hole interaction $\tilde{V}_{p\text{-}h}(q)$ through the sum rule Eq. (1.4) from the static structure function.

The proof of the m_1 sum rule is identical to the one for bosons. Due to the symmetry

$$\chi(q;\omega) = \chi^*(q;-\omega)$$

we can write

$$m_1 = -\frac{1}{2\pi}\Im m\int_{-\infty}^{\infty} d(\hbar\omega)\hbar\omega\chi(q;\omega). \tag{E1}$$

All poles of $\chi(q;\omega)$ are in the lower half plane, allowing to close the integral in the upper half plane. For large ω we have, however,

$$\chi_0(q;\omega) - \chi^{RPA}(q;\omega) \propto \omega^{-4}, \tag{E2}$$

$$\chi_0(q;\omega) - \chi(q;\omega) \propto \omega^{-4} \tag{E3}$$

since

$$\tilde{V}_{A,B}(q;\omega) = \tilde{V}_{p\text{-}h}(q) + \frac{\text{const}}{\omega} \quad \text{as} \quad \omega\to\infty. \tag{E4}$$

We have therefore

$$\Im m\int_{-\infty}^{\infty} d(\hbar\omega)\hbar\omega\chi(q;\omega) = \Im m\int_{-\infty}^{\infty} d(\hbar\omega)\hbar\omega\chi^{RPA}(q;\omega) = \Im m\int_{-\infty}^{\infty} d(\hbar\omega)\hbar\omega\chi(q;\omega). \tag{E5}$$

For fermions, the frequency integration in Eq. (1.4) must be carried out numerically, which is best done by Wick rotation along the imaginary axis. The result of the integration is no longer rigorously independent of the approximation used for the response function.

Figure 14 compares the m_0 sum rule calculated within the RPA and the pair-excitation theory. Evidently, the discrepancy is very small. One can understand by comparing with the boson theory: If we restricted the fluctuation operators $\delta u^{(1)}_{ph}(t)$ and $\delta u^{(2)}_{pp'hh'}(t)$ to be functions of momentum trans-

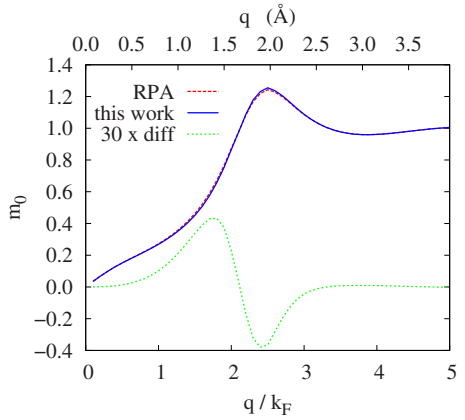

FIG. 14. (Color online) Result of the m_0 sum rule for ^{3}He at saturated vapor pressure. The purple dashed line shows the FHNC $S(q)$ and the blue short dashed line the result from the pair-fluctuation theory; the dashed green line shows the difference, magnified by a factor of 30 to make it visible.

fers $\mathbf{q}=\mathbf{p}-\mathbf{h}$ and $\mathbf{q}'=\mathbf{p}'-\mathbf{h}'$, we would end up with a density-density response function that is formally identical to that of bosons and would, hence, lead to an $S(q)$ that is independent of the treatment of the pair fluctuations. The expectation that the inclusion of the particle-hole structure of the two-pair-energy denominator makes only a small difference is verified in Fig. 14. Thus, it is also legitimate in the pair-excitation theory to obtain the static particle-hole interaction $\tilde{V}_{\text{p-h}}(q)$ from the static structure function $S(q)$ through Eqs. (1.4) and (1.7).

APPENDIX F: IMPLEMENTATION RECIPE

This section provides, for the convenience of the reader and easy further reference, a compilation of all necessary ingredients to implement the theory. Mostly a summary of Secs. IV and V A, we deliberately refrain from any explanation to avoid redundancy and keep it as compact as possible.

We have shown in our applications to ^{3}He and the electron liquid that for practical purposes, only one of the local three-body vertices is necessary:

$$\tilde{K}_{q,q'q''}=\frac{\hbar^2}{2m}\frac{S(q')S(q'')}{S_{\text{F}}(q)S_{\text{F}}(q')S_{\text{F}}(q'')}[\mathbf{q}\cdot\mathbf{q}'\tilde{X}_{\text{dd}}(q')+\mathbf{q}\cdot\mathbf{q}''\tilde{X}_{\text{dd}}(q'')-q^2\tilde{u}_3(q,q',q'')], \tag{F1}$$

where $u_3(q,q',q'')$ is the three-body ground-state correlation.[28] The effective interaction $\tilde{W}_{\text{A}}(q,\omega)$ is then

$$\tilde{W}_{\text{A}}(q;\omega)=\frac{1}{2N}\sum_{\mathbf{q}'\mathbf{q}''}|\tilde{K}_{q,q'q''}|^2\tilde{E}^{-1}(q',q'';\omega) \tag{F2}$$

whereas $\tilde{W}_{\text{B}}(q,\omega)$ vanishes. Consequently, the components of the (energy-dependent) interaction matrix $\mathbf{V}_{\text{p-h}}(\omega)$ are

$$\tilde{V}_{\text{A}}(q;\omega)=\tilde{V}_{\text{p-h}}(q)+[\sigma_q^+]^2\tilde{W}_{\text{A}}(q;\omega)+[\sigma_q^-]^2\tilde{W}_{\text{A}}^*(q;-\omega), \tag{F3}$$

$$\tilde{V}_{\text{B}}(q;\omega)=\tilde{V}_{\text{p-h}}(q)+\sigma_q^+\sigma_q^-[\tilde{W}_{\text{A}}(q;\omega)+\tilde{W}_{\text{A}}^*(q;-\omega)] \tag{F4}$$

with $\sigma_q^{\pm}\equiv[S_{\text{F}}(q)\pm S(q)]/2S(q)$.

Finally we need the pair propagator

$$\tilde{E}^{-1}(q_1,q_2;\omega)=-\int_{-\infty}^{\infty}\frac{d(\hbar\omega')}{2\pi i}\kappa(q_1;\omega')\kappa(q_2;\omega-\omega'), \tag{F5}$$

$$\kappa(q;\omega)=\frac{\kappa_0(q;\omega)}{1+\hbar\omega\tilde{\Gamma}_{\text{dd}}(q)\kappa_0(q;\omega)} \tag{F6}$$

with the partial Lindhard function

$$\kappa_0(q;\omega)\equiv\frac{1}{N}\sum_h\frac{\bar{n}_{\mathbf{p}}n_{\mathbf{h}}}{\hbar\omega-e_{ph}+i\eta} \tag{F7}$$

The simplifications of the interactions do not significantly simplify the form Eq. (5.7) of the density-density response function.

[1] A. K. Kerman and S. E. Koonin, Ann. Phys. (N.Y.) **100**, 332 (1976).
[2] P. Kramer and M. Saraceno, *Geometry of the Time-Dependent Variational Principle in Quantum Mechanics*, Lecture Notes in Physics Vol. 140 (Springer, Berlin, New York, 1981).
[3] D. J. Thouless, *The Quantum Mechanics of Many-Body Systems*, 2nd ed. (Academic Press, New York, 1972).
[4] J. M. C. Chen, J. W. Clark, and D. G. Sandler, Z. Phys. A **305**, 223 (1982).
[5] E. Krotscheck, Phys. Rev. A **26**, 3536 (1982).
[6] H. W. Jackson and E. Feenberg, Ann. Phys. (N.Y.) **15**, 266 (1961).
[7] C. E. Campbell and E. Krotscheck, Phys. Rev. B **80**, 174501 (2009).
[8] L. D. Landau, Sov. Phys. JETP **3**, 920 (1957).
[9] L. D. Landau, Sov. Phys. JETP **5**, 101 (1957).
[10] R. P. Feynman, Phys. Rev. **94**, 262 (1954).
[11] R. P. Feynman and M. Cohen, Phys. Rev. **102**, 1189 (1956).
[12] H. W. Jackson and E. Feenberg, Rev. Mod. Phys. **34**, 686 (1962).
[13] E. Feenberg, *Theory of Quantum Fluids* (Academic, New York, 1969).
[14] H. W. Jackson, Phys. Rev. A **4**, 2386 (1971).
[15] H. W. Jackson, Phys. Rev. A **8**, 1529 (1973).
[16] H. W. Jackson, Phys. Rev. A **9**, 964 (1974).
[17] C. C. Chang and C. E. Campbell, Phys. Rev. B **13**, 3779 (1976).
[18] C. E. Campbell and E. Krotscheck (unpublished).
[19] C. H. Aldrich III and D. Pines, J. Low Temp. Phys. **32**, 689

(1978).
[20] N. Iwamoto and D. Pines, Phys. Rev. B **29**, 3924 (1984).
[21] J. W. Clark, in *Progress in Particle and Nuclear Physics*, edited by D. H. Wilkinson (Pergamon Press, Oxford, 1979), Vol. 2, pp. 89–199.
[22] A. Fabrocini, S. Fantoni, and E. Krotscheck, *Introduction to Modern Methods of Quantum Many-Body Theory and their Applications, Advances in Quantum Many-Body Theory* (World Scientific, Singapore, 2002), Vol. 7.
[23] R. Scherm, K. Guckelsberger, B. Fåk, K. Sköld, A. J. Dianoux, H. Godfrin, and W. G. Stirling, Phys. Rev. Lett. **59**, 217 (1987).
[24] B. Fåk, K. Guckelsberger, R. Scherm, and A. Stunault, J. Low Temp. Phys. **97**, 445 (1994).
[25] H. R. Glyde, B. Fåk, N. H. van Dijk, H. Godfrin, K. Guckelsberger, and R. Scherm, Phys. Rev. B **61**, 1421 (2000).
[26] C. Sternemann, S. Huotari, G. Vankó, M. Volmer, G. Monaco, A. Gusarov, H. Lustfeld, K. Sturm, and W. Schülke, Phys. Rev. Lett. **95**, 157401 (2005).
[27] S. Huotari, C. Sternemann, W. Schülke, K. Sturm, H. Lustfeld, H. Sternemann, M. Volmer, A. Gusarov, H. Müller, and G. Monaco, Phys. Rev. B **77**, 195125 (2008).
[28] E. Krotscheck, J. Low Temp. Phys. **119**, 103 (2000).
[29] A. D. Jackson, A. Lande, and R. A. Smith, Phys. Rep. **86**, 55 (1982).
[30] P. M. Morse and H. Feshbach, *Methods of Theoretical Physics* (McGraw-Hill, New York, Toronto, London, 1953), Vol. I.
[31] E. Krotscheck and J. W. Clark, Nucl. Phys. A **328**, 73 (1979).
[32] E. Krotscheck, in *Introduction to Modern Methods of Quantum Many-Body Theory and their Applications, Advances in Quantum Many-Body Theory*, edited by A. Fabrocini, S. Fantoni, and E. Krotscheck (World Scientific, Singapore, 2002), Vol. 7, pp. 267–330.
[33] D. M. Ceperley and B. J. Alder, Phys. Rev. Lett. **45**, 566 (1980).
[34] J. Casulleras and J. Boronat, Phys. Rev. Lett. **84**, 3121 (2000).
[35] E. Krotscheck, Ann. Phys. (N.Y.) **155**, 1 (1984).
[36] V. Apaja, J. Halinen, V. Halonen, E. Krotscheck, and M. Saarela, Phys. Rev. B **55**, 12925 (1997).
[37] A. Holas, *Strongly Coupled Plasma Physics* (Plenum Press, New York, 1986), pp. 463–482.
[38] G. Giuliani and G. Vignale, *Quantum Theory of the Electron Liquid* (Cambridge University Press, Cambridge, 2005).
[39] C. E. Campbell and E. Krotscheck, J. Low Temp. Phys. **158**, 226 (2010).
[40] H. Glyde, *Excitations in Liquid and Solid Helium* (Oxford University Press, Oxford, 1994).
[41] F. Albergamo, R. Verbeni, S. Huotari, G. Vankó, and G. Monaco, Phys. Rev. Lett. **99**, 205301 (2007).
[42] A. J. M. Schmets and W. Montfrooij, Phys. Rev. Lett. **100**, 239601 (2008).
[43] F. Albergamo, R. Verbeni, S. Huotari, G. Vankó, and G. Monaco, Phys. Rev. Lett. **100**, 239602 (2008).
[44] D. Pines, Phys. Today **34**(11), 106 (1981).
[45] V. K. Mishra, G. E. Brown, and C. J. Pethick, J. Low Temp. Phys. **52**, 379 (1983).
[46] G. E. Brown, C. J. Pethick, and A. Zaringhalam, J. Low Temp. Phys. **48**, 349 (1982).
[47] B. L. Friman and E. Krotscheck, Phys. Rev. Lett. **49**, 1705 (1982).
[48] E. Krotscheck and J. Springer, J. Low Temp. Phys. **132**, 281 (2003).
[49] N.-H. Kwong, Ph.D. thesis, California Institute of Technology, 1982.
[50] M. Panholzer, H. M. Böhm, R. Holler, and E. Krotscheck, J. Low Temp. Phys. **158**, 135 (2010).
[51] R. A. Aziz, F. R. W. McCourt, and C. C. K. Wong, Mol. Phys. **61**, 1487 (1987).
[52] D. S. Greywall, Phys. Rev. B **33**, 7520 (1986).
[53] R. de Bruyn Ouboter and C. N. Yang, Physica B & C **144**, 127 (1986).
[54] S. Moroni, D. M. Ceperley, and G. Senatore, Phys. Rev. Lett. **69**, 1837 (1992).
[55] F. Caupin, J. Boronat, and K. H. Andersen, J. Low Temp. Phys. **152**, 108 (2008).
[56] S. Moroni, D. M. Ceperley, and G. Senatore, Phys. Rev. Lett. **75**, 689 (1995).
[57] K. S. Singwi and M. P. Tosi, Solid State Phys. **36**, 177 (1982).
[58] H. M. Böhm, R. Holler, E. Krotscheck, and M. Panholzer, J. Phys. A: Math. Theor. **42**, 214037 (2009).
[59] K. Sturm and A. Gusarov, Phys. Rev. B **62**, 16474 (2000).
[60] M. Corradini, R. DelSole, G. Onida, and M. Palummo, Phys. Rev. B **57**, 14569 (1998).
[61] N. Iwamoto, E. Krotscheck, and D. Pines, Phys. Rev. B **29**, 3936 (1984).
[62] D. S. Greywall, Phys. Rev. B **27**, 2747 (1983).
[63] J. Boronat, J. Casulleras, V. Grau, E. Krotscheck, and J. Springer, Phys. Rev. Lett. **91**, 085302 (2003).
[64] E. Krotscheck and M. L. Ristig, Phys. Lett. A **48**, 17 (1974).